NAVAL POSTGRADUATE SCHOOL

MONTEREY, CALIFORNIA

THESIS

EVALUATION AND ANALYSIS OF DDG-81 SIMULATED ATHWARTSHIP SHOCK RESPONSE

by

Douglas C. Petrusa

June 2004

Thesis Advisor: Young S. Shin

Approved for public release; distribution is unlimited

THIS PAGE INTENTIONALLY LEFT BLANK

REPORT DOCUMENTATION PAGE			Form Approved OMB No. 0704-0188
Public reporting burden for this collection of information is estimated to average 1 hour per response, including the time for reviewing instruction, searching existing data sources, gathering and maintaining the data needed, and completing and reviewing the collection of information. Send comments regarding this burden estimate or any other aspect of this collection of information, including suggestions for reducing this burden, to Washington headquarters Services, Directorate for Information Operations and Reports, 1215 Jefferson Davis Highway, Suite 1204, Arlington, VA 22202-4302, and to the Office of Management and Budget, Paperwork Reduction Project (0704-0188) Washington DC 20503.			
1. AGENCY USE ONLY *(Leave blank)*	**2. REPORT DATE** June 2004	**3. REPORT TYPE AND DATES COVERED** Master's Thesis	
4. TITLE AND SUBTITLE: Evaluation and Analysis of DDG-81 Simulated Athwartship Shock Response			**5. FUNDING NUMBERS**
6. AUTHOR(S) Douglas C. Petrusa			
7. PERFORMING ORGANIZATION NAME(S) AND ADDRESS(ES) Naval Postgraduate School Monterey, CA 93943-5000			**8. PERFORMING ORGANIZATION REPORT NUMBER**
9. SPONSORING /MONITORING AGENCY NAME(S) AND ADDRESS(ES) N/A			**10. SPONSORING/MONITORING AGENCY REPORT NUMBER**
11. SUPPLEMENTARY NOTES The views expressed in this thesis are those of the author and do not reflect the official policy or position of the Department of Defense or the U.S. Government.			
12a. DISTRIBUTION / AVAILABILITY STATEMENT Approved for public release; distribution is unlimited			**12b. DISTRIBUTION CODE**

13. ABSTRACT (maximum 200 words)

In 2001 the USS WINSTON CHURCHILL (DDG-81) was subjected to three underwater explosions as part of a ship shock trial. Using the actual trial data from experiment and three-dimensional dynamic models of the ship and surrounding fluid very successful comparisons of the vertical motion have been achieved. On average, the magnitude of the vertical motion is three to four times the magnitude of athwartship motion. Previous simulations of this athwartship motion have been less accurate than the vertical motion simulations.

This thesis examines recent efforts attempted to improve the simulation results of the athwartship motion including shock spectra analysis, and the reasons behind the disparities that exist between the simulated values and the actual trial data.

14. SUBJECT TERMS Underwater Explosion, UNDEX, Modeling and Simulation, Shock and Vibration, Ship Shock, Athwartship Shock Response, Shock Spectra, USS Winston S. Churchill, DDG-81			**15. NUMBER OF PAGES** 90
			16. PRICE CODE
17. SECURITY CLASSIFICATION OF REPORT Unclassified	**18. SECURITY CLASSIFICATION OF THIS PAGE** Unclassified	**19. SECURITY CLASSIFICATION OF ABSTRACT** Unclassified	**20. LIMITATION OF ABSTRACT** UL

NSN 7540-01-280-5500 Standard Form 298 (Rev. 2-89)
Prescribed by ANSI Std. 239-18

THIS PAGE INTENTIONALLY LEFT BLANK

Approved for public release; distribution is unlimited

EVALUATION AND ANALYSIS OF DDG-81 SIMULATED ATHWARTSHIP SHOCK RESPONSE

Douglas C. Petrusa
Lieutenant, United States Coast Guard
B.S., US Merchant Marine Academy, 1997

Submitted in partial fulfillment of the
requirements for the degree of

MASTER OF SCIENCE IN MECHANICAL ENGINEERING

from the

NAVAL POSTGRADUATE SCHOOL
June 2004

Author: Douglas C. Petrusa

Approved by: Dr. Young S. Shin
Thesis Advisor

Dr. Anthony Healey
Chairman, Department of Mechanical and Astronautical Engineering

THIS PAGE INTENTIONALLY LEFT BLANK

ABSTRACT

In 2001 the USS WINSTON CHURCHILL (DDG-81) was subjected to three underwater explosions as part of a ship shock trial. Using the actual trial data from experiment and three-dimensional dynamic models of the ship and surrounding fluid very successful comparisons of the vertical motion have been achieved. On average, the magnitude of the vertical motion is three to four times the magnitude of athwartship motion. Previous simulations of this athwartship motion have been less accurate than the vertical motion simulations.

This thesis examines recent efforts attempted to improve the simulation results of the athwartship motion including shock spectra analysis, and the reasons behind the disparities that exist between the simulated values and the actual trial data.

THIS PAGE INTENTIONALLY LEFT BLANK

TABLE OF CONTENTS

LIST OF FIGURES

THIS PAGE INTENTIONALLY LEFT BLANK

LIST OF TABLES

THIS PAGE INTENTIONALLY LEFT BLANK

ACKNOWLEDGEMENTS

I would like to thank Professor Shin and Jake Didoszak for their support and assistance from start to finish in this thesis process. I am also very thankful to the staff in at UERD, especially Fred Costanzo who personally tutored me in mechanical vibrations and Steve Rutgerson who helped shed the light on certain numerical aspects of the sensor data.

ENS Lau and ENS Fensterer, for being able to help develop and compare models, debug computer programs and restore lost and missing data from computer crashes. This research would have taken years without your help.

To my wife Debbie and son Kyle, who have supported me, encouraged me and most importantly been patient with me as I have spent many days away from you conducting this work.

THIS PAGE INTENTIONALLY LEFT BLANK

I. INTRODUCTION

A. BACKGROUND

Great research has been accomplished in the field of underwater explosions (UNDEX) since World War II. Surface ships and submarines were subjected to damage caused by mines, depth charges and torpedoes throughout the war. Direct contact with such ordinance was not required for major damage to occur. The requirement to be able to predict and reduce damage to a ship's hull from an UNDEX event was evident. The US Navy has been performing live fire ship shock trials over the years in accordance with OPNAVINST 9072.2 [Ref. 1], NAVSEA 0908-LP-000-3010A [Ref. 2] and MIL-S-901D [Ref. 3] to observe the UNDEX phenomenon and its effects on existing NAVY ships.

The lead ship of each class is subjected to these trials, and subsequent trials are conducted at the discretion of the CNO to validate corrective actions taken from deficiencies identified in the first trial, to validate changes to a class of ship not represented in the first trial, or to validate the work of different shipbuilders. Due to major upgrades to the Arleigh Burke guided missile destroyer (DDG) class, the USS WINSTON CHURCHILL (DDG-81) underwent these ship shock trials in May and June of 2001. Three separate explosions at various distances were conducted, and with the use of over six hundred sensors located throughout the ship, the dynamic response to the UNDEX was recorded.

Computer modeling has been utilized to predict many of the aspects from an UNDEX event. Also, the finite element method has become a standard among engineers to calculate dynamic responses in complex structures. Combining these two theories, finite element models of a ship and its surrounding fluid have been subjected to virtual attacks. These UNDEX simulations have been remarkably accurate in predicting the early time vertical response when compared to the actual ship shock trial data collected.

With just a few keystrokes the geometry of a charge may be changed, or the physical amount of charge may be increased. Without harm to crew, hull, mechanical, electrical systems and to the marine environment a plethora of conditions can easily be modified. While only three explosions were conducted with DDG-81, the uses of these

simulations show incredible potential. In addition, computer technology advances have greatly reduced the amount of time required to perform these simulations. However, there are still areas where the simulation results do not match the actual trial data. In particular, the athwartship motion has yet to be modeled with as great success as the vertical motion.

In the near future these virtual models will be more accurate, run faster, and perhaps eliminate the need for live fire testing. The ability to predict and correct weaknesses in a particular hull design before a ship is built shows unlimited potential for the future in terms of cost savings and operational readiness.

B. SCOPE OF RESEARCH

Using the techniques developed at the Naval Postgraduate School and with actual ship shock trial data collected in May and June of 2001 of the USS WINSTON CHURCHILL (DDG-81), this thesis serves to further the research conducted by Schneider [Ref. 4] and Didoszak [Ref. 5]. Model refinement and comparative analysis of the vertical and athwartship velocity response have been the basis of these previous studies. This thesis will further examine the athwartship velocity response and present shock spectra analysis. Data processing techniques will also be examined along with reasons behind the disparities that exist between the simulated values and the actual trial data.

II. SHIP SHOCK MODELING

A. FINITE ELEMENT MODEL

Two finite element models of Arleigh Burke Class Destroyers were created by Gibbs and Cox, Inc. [Ref 6] to assist with the ship shock modeling effort. Modifications made to this class of ship are known as the Flight IIA DDG's. The USS WINSTON CHURCHILL (DDG-81) was modeled in far greater detail than the previous finite element model USS John Paul Jones (DDG-53) as shown below in Table 1.

Model Summary	DDG-53	DDG-81
Number of Nodes	35,216	40,513
Degrees of Freedom (6 per node)	211,296	243,078
Shell Elements	41,078	48,603
Bar and Beam Elements	42,659	49,968
Discrete Elements	416	416
Rigid Elements	55	55

Table 1. Finite Element Model Specifics Comparison [From Ref 6.]

Some of the major modifications to this ship class include the following:

- Installation of Dual Helicopter hangers
- Extension of the Transom by five feet
- Replacement of the five inch 54 caliber gun with a five inch 62 cailber gun
- Removal of forward and aft VLS cranes and installation of 6 new VLS cells
- Addition of five blast hardened bulkheads

As shown in Figure 1, the physical differences between the DDG's are apparent. Thus, shock trials needed to be conducted in keeping with OPNAVISNT 9072.2 [Ref. 1].

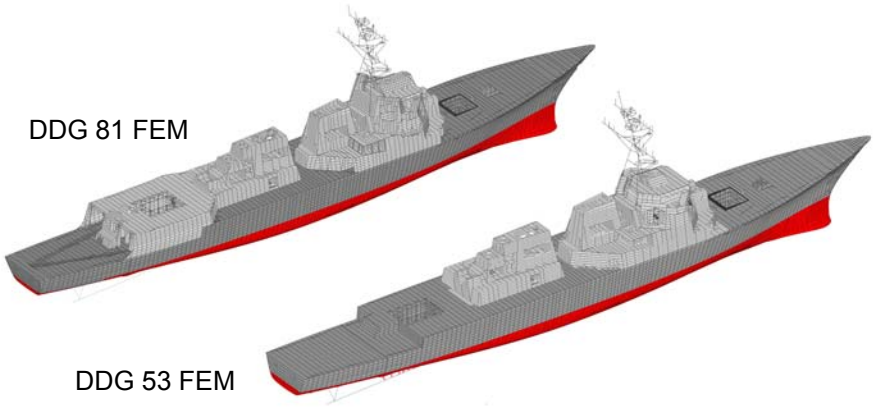

Figure 1. DDG-81 (top) and DDG-53 (bottom) Finite Element Models [From Ref. 6]

These models were generated in a MSC NASTRAN compatible environment and were validated by performing physical checks onboard each of the vessels. Different techniques were used in the DDG-81 model that served to improve model and simulation accuracy, when compared to earlier models. For example, instead of smearing mass across the model the actual DDG-81 weight database (weight-tapes) was incorporated. Much of the finite element model was generated with the use of Computer Aided Drawing (CAD) blueprints of the vessel. This technique enabled the model to be built much more quickly and far more precise than the DDG-53 model. Also, the liquid load, ordinance, cargo and personnel loads during each explosion was calculated and incorporated into the model. Since there were three explosions, or three "Shots," three separate finite element models of DDG-81 were used in the simulations.

Figure 2, shows clearly the great amount of detail involved with the DDG-81 finite element model. The nominal mesh size of this model is 27 inches by 48 inches. However, Combat Information Center (CIC) was modeled with a finer mesh density due to the amount of sensitive electronics, allowing a more detailed analysis of that particular compartment.

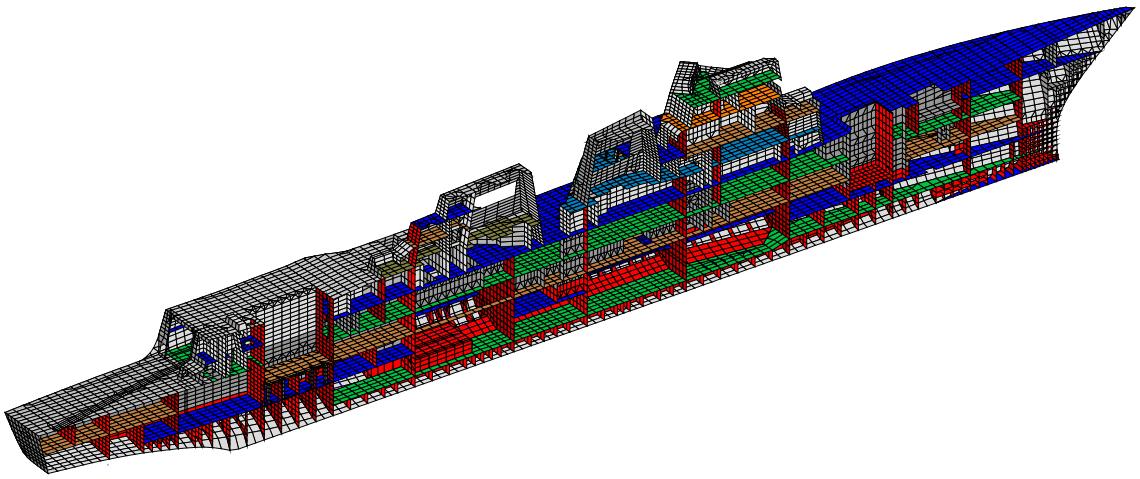

Figure 2. Centerline cutaway view of DDG-81 (port side) Finite Element Model [From Ref. 6]

B. FLUID MESH

The fluid mesh is the finite element model of the water that surrounds the ship model. Created at the Naval Postgraduate School (NPS) by Hart [Ref. 8] and Schneider [Ref. 4], this mesh is essential for the simulation of an UNDEX event with LS-DYNA/USA software. Using TrueGrid, a mesh-generating program, the wetted surface of the DDG-81 finite element model was extruded into a finite element model of its own. Figure 3 shows the fluid inner liner, which is orthogonal along the wetted surface of the ship with the exception of the waterline and liner seams. The liner seams exist since areas such as the sonar dome, keel, bow and stern that have complex shapes. These seams have been smoothed by adding curved wedges to prevent gaps. At only seven inches thick this inner liner serves as the foundation for additional fluid mesh layers.

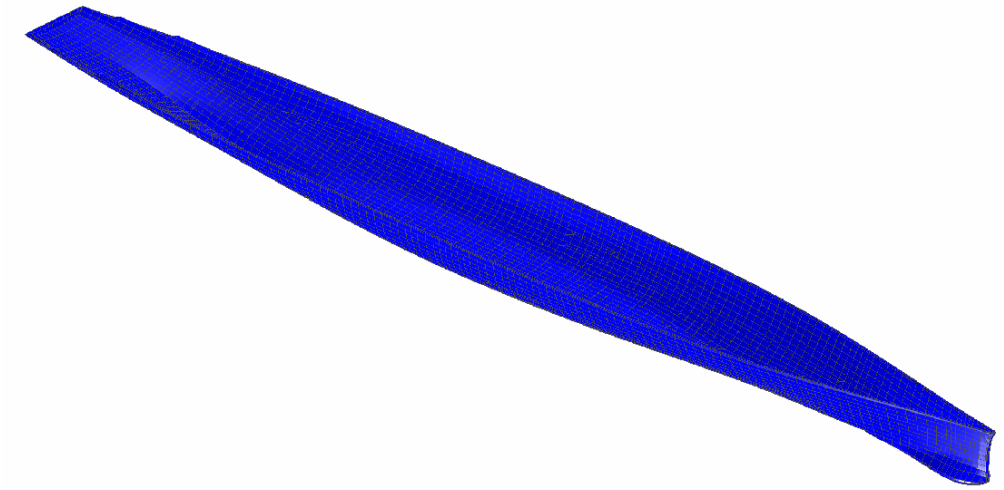

Figure 3. Thin Fluid Mesh Inner Liner [From Ref. 8]

The next layer of the fluid mesh liner is an additional eight inches thick. The combined two-layer inner mesh ensures that the critical element thickness of nine inches required by the Underwater Shock Analysis Code (USA) is not exceeded. This combined mesh also establishes the waterline at 21.5 feet. Although additional layers were added to this mesh, it was at this point that the virtual modeling could begin. The additional layers are known as the inner mesh, transitional fluid mesh, and outer fluid mesh.

Comprehensive studies conducted by Hart [Ref. 8] and Schneider [Ref. 4] varied the ultimate depth of the outer fluid mesh. Results of their simulations have shown that the combined fluid mesh must reach the bottom of the lower cavitation boundary. Figure 4 shows the coupled model with the various layers of the fluid mesh.

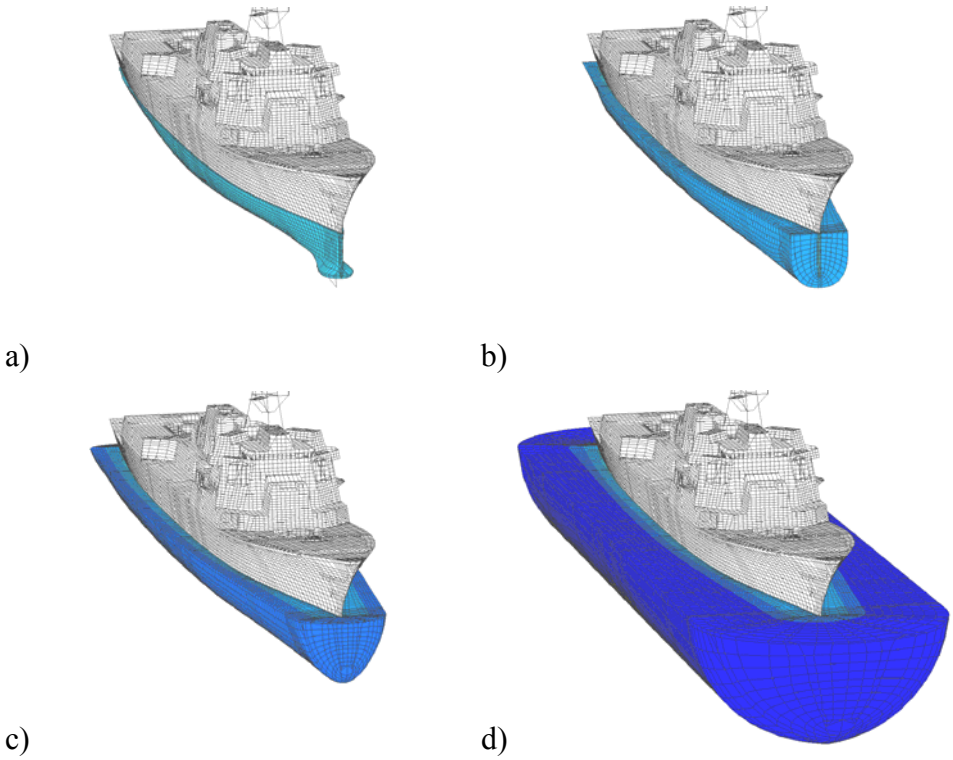

Figure 4. Fluid Mesh Layers: Inner Liner (a), Inner Mesh (b), Transitional Mesh (c), Outer Mesh (d) [From Ref. 7]

C. NODE IDENTIFICATION AND SELECTION

Previous simulations in the Shock and Vibrations Computational Lab (SVCL) at NPS examined the same series of thirty-two nodes from within the finite element model. Although these nodes represented a variety of areas of interest from the entire ship, this study focused more attention on choosing the specific nodes that matched the exact locations of the sensors. This was performed so that that the motion simulated in this study could be compared to actual trial data without any doubt.

Having been provided with a list of three-dimensional coordinates for each nodes in the DDG-81 finite element model from Gibbs and Cox [Ref. 10] and a list of the three-dimensional coordinates of each dynamic sensor from NAVSEA [Ref. 11] the task of matching these positions took place. With over 600 sensors locations and over 175,000 total nodes (combined ship and fluid model) a computer program was written to perform this task.

All of the nodes, sensors, and respective coordinates were input in ASCII format into a MATLAB script file. At this point the three-dimensional distance formula was applied to calculate the distance between each sensor with every single node. This data was stored in a vector, and an iterative command commenced the same task for the next sensor. When completed, a matrix of data was stored holding all of the distances between every node and every sensor. MATLAB's built-in min command was then used to locate the least distance between each sensor and each node.

With this data, the best pair of nodes and sensors were matched. There exists other methods of performing this task, but this method seemed to provide the best results. For example, had a weighted averaging technique been applied to a cube of eight nodes containing one sensor, the simulations would have been adversely prolonged. All of the nodes analyzed in this study were less than eight inches away from the location of the sensors. In comparison, the previous studies node selection criteria was based on locations within the nominal mesh size of a sensor's location. This allowed for node selection with distances as great as 48 inches from its corresponding sensor.

D. SIMULATING UNDEX WITH LS-DYNA/USA

LS-DYNA is an industry standard finite element analysis program that is capable of three-dimensional non-linear dynamic analysis using explicit time integration algorithms. Underwater Shock Analysis Code (USA) is a series of complex algorithms that approximate the fluid behavior in an UNDEX event. These two programs have been combined into one powerful tool that generates a six degree of freedom dynamic analysis to a floating or submerged structure. Due to the fact that the physics of underwater explosions is rather complex, a concise background of this phenomenon will be described.

1. UNDEX Phenomenon

There is a defined sequence that occurs during an UNDEX event. The first of which is the incident pressure wave or incident shock wave. This is known as a shock wave due to the fact that the pressure waves velocity exceeds the acoustic velocity of

water. The shock waves energy propagates through the water under extreme pressure. This pressure can easily be calculated at any point, as long as the point is located between 10 and 100 times the charge radius away from the charge location. The USA code effectively calculates the incident pressure wave.

When the shock wave reaches the free surface, it becomes reflected as a tensile pressure wave. Using an image charge positioned above the waterline symmetrically from the actual charge the tensile wave can be modeled. Figure 5 shows the how the image charge is utilized. Mathematically, the sum of the pressure wave and the tension wave would yield a negative value over a large area. However, since water does not sustain tension cavitation occurs. This is commonly known as the bulk cavitation effect. Properly calculating this bulk cavitation zone is essential to modeling an UNDEX event. Figure 6 shows the bulk cavitation zone of a 10,000-pound HBX-1 charge. Local cavitation also occurs at the interface between the fluid and structure.

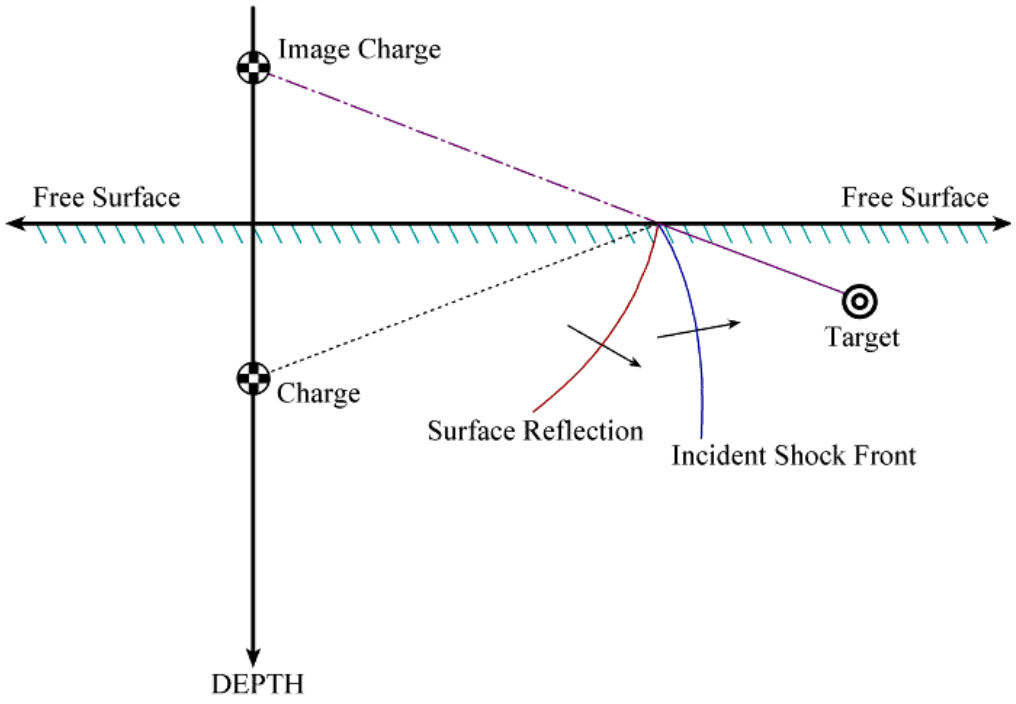

Figure 5. Charge and Image Charge Positioning [From Ref. 9]

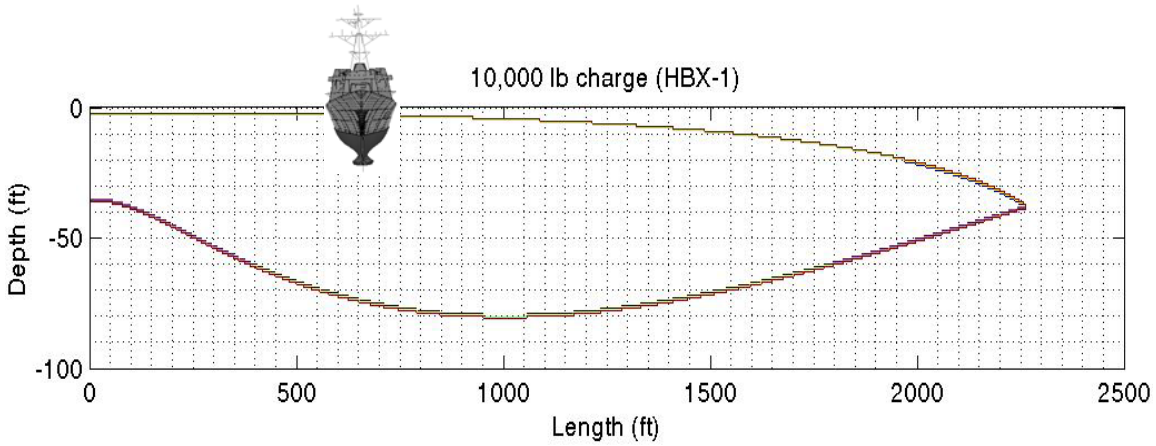

Figure 6. Bulk Cavitation Zone (not to scale)

An explosive gas bubble created upon detonation will expand rapidly underwater. Unlike an explosion in air, the pressure inside of the gas bubble will reach equilibrium with the hydrostatic pressure of the surrounding fluid. The radius of the bubble will naturally increase until this equilibrium is reached, and momentum will cause the bubble radius to continue to increase beyond equilibrium. At it's maximum radius the bubble will collapse due to the positive pressure gradient between the bubble and surrounding fluid. At this point the bubble is small, yet a negative pressure gradient exists between the bubble and surrounding fluid causing the bubble to expand again towards equilibrium. Depending on the depth and size of the charge this bubble oscillation will continue to occur as it migrates toward the surface and as the energy is dissipated into the surrounding fluid.

2. Simulating UNDEX with USA

Using a Doubly Asymptotic Approximation (DAA) the USA code calculates the fluid structure interaction during the UNDEX. This method is extremely effective at approximating the early time (high-frequency) response and late time (low-frequency) response [Ref. 12]. Starting with the second order linear equation of motion

$$[M]\{\ddot{x}\}+[C]\{\dot{x}\}+[K]\{x\} = \{f\} \quad (1)$$

where [M], [C], and [K] are the mass, damping, and stiffness matrices respectively. The Force vector {f} is defined as

$$\{f\} = -[G][A_f]\{(p_I + p_S)\} + \{f_D\} \tag{2}$$

where [G] is the transformation matrix that relates the structural and fluid surface forces, $[A_f]$ is a diagonal area matrix pertaining to the fluid elements, $\{p_I\}$ and $\{p_S\}$ are the incident and pressure wave vectors, and $\{f_D\}$ is the dry structure applied force vector.

Having a defined equation of motion is essential to calculating the dynamic response to this or any finite element model. DAA utilizes the structural equation of motion and a fluid particle equation of motion shown below

$$[M_f]\{\dot{p}_s\} + \rho c[A_f]\{p_s\} = \rho c[M_f]\{\dot{u}_s\} \tag{3}$$

where $[M_f]$ is the mass matrix of the fluid mesh, and $\{u_S\}$ is the scattered-wave fluid particle velocity vector. The following equation utilizes the transformation matrix described in equation (2) to relate the fluid particle velocities and the structural response.

$$[G]^T\{\dot{x}\} = \{u_I\} + \{u_S\} \tag{4}$$

Combining equations (1) through (4) the following two equations are formed.

$$[M]\{\ddot{x}\} + [C]\{\dot{x}\} + [K]\{x\} = -[G][A_f]\{(p_I + p_S)\} \tag{5}$$

$$[M_f]\{\dot{p}_S\} + \rho c[A_f]\{p_S\} = \rho c[M_f]([G]^T\{\ddot{x}\} - \{\dot{u}_I\}) \tag{6}$$

The USA code solves these systems of equations for the forces at the fluid structure interface. Knowing these forces, finite element analysis software may be then used to calculate the structural response. Using the following three programs within USA the shock wave is generated and the DAA method is used to calculate the forces:

- FLUMAS – Generates the fluid mass matrix and the pressure from the spherical shock wave [Ref. 13]
- AUGMAT – Takes data from FLUMAS and assembles the DAA matrices in preparation for solution [Ref. 13]

- TIMINT – Conducts a step by step numerical time integration using the DAA method [Ref. 13]

3. Finite Element Analysis

Prior to any simulation effort the mass, damping, and stiffness matrices need to be determined. The structural model and shock trial data of DDG-53 led to extensive research conducted at NPS in proportional damping. Finite element analysis software may be very powerful, but it requires linear symmetrical matrices. Unlike the mass and stiffness matrices, which are easily developed from material properties, the damping matrix must be approximated so that the property of orthogonality holds true. If it is not orthogonal a consistent damping coefficient may not be used. Using proportional damping the matrix [C] from equation (1) is approximated by a linear combination of the mass and stiffness matrices as shown below

$$[C] = \alpha[M] + \beta[K] \tag{7}$$

Since the mass and stiffness matrices are symmetric, a linear combination of the two matrices would also be symmetric. The coefficients alpha and beta were not calculated with ease, months of research of actual shock trail data was utilized with least squares curve fitting techniques to calculate their values. Yet once established these coefficients serve to form an approximation of the damping matrix that may now be diagonalizable using orthogonality. The coefficients determined in DDG-53 were used in the DDG-81 simulation [Ref. 14].

LS-DYNA was used to calculate the structural response to this combined ship and fluid model. The DDG-81 model was developed in a MSC NASTRAN compatible environment and subsequently was converted into a keyword format for LS-DYNA processing at NPS. The following figure depicts the entire simulation process.

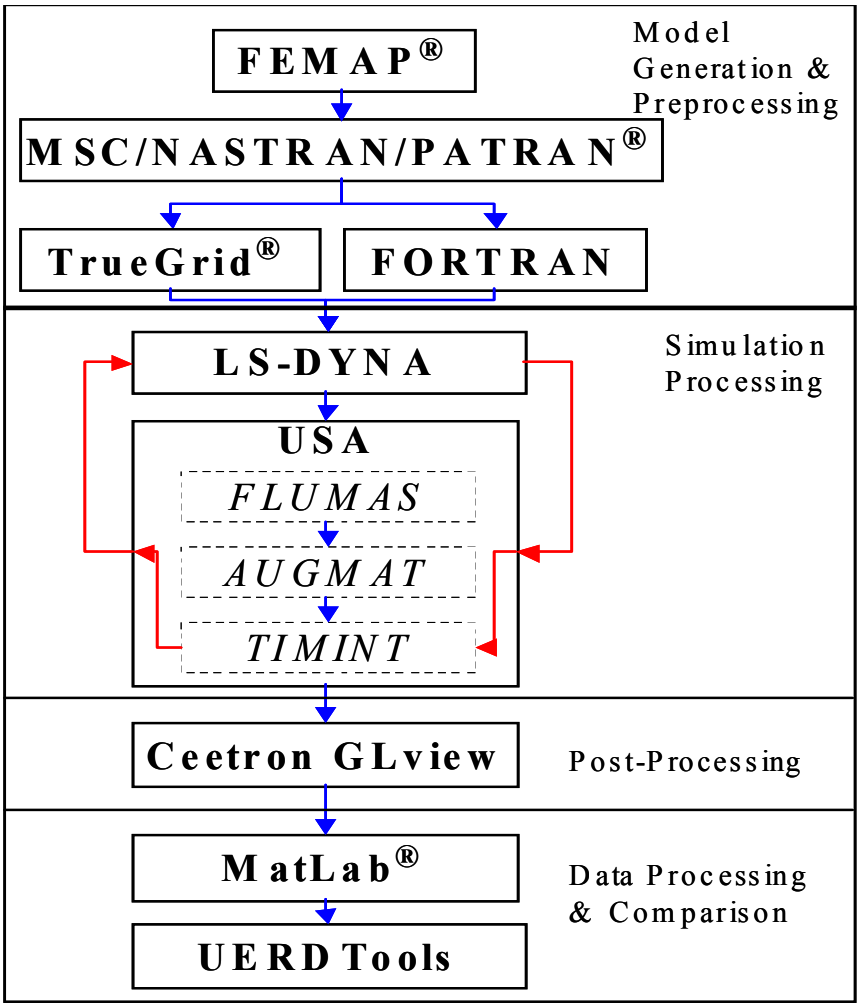

Figure 7. Simulation Process Flowchart [From Ref. 4]

LS-DYNA is capable of performing many kinds of analysis including plastic deformation, and is widely used in the automotive industry for crash test simulations. However, all of the simulations presented in this study are using elastic material properties. Six degree of freedom analysis is conducted, and using post-processing and viewing software such as Ceetron Glview nodal displacement, velocity, and acceleration vectors can easily be exported and plotted.

THIS PAGE INTENTIONALLY LEFT BLANK

III. ATHWARTSHIP RESPONSE

Although much smaller in magnitude when compared to the vertical response, as shown in Figure 8, the athwartship response is still a very important aspect to shock and vibrations community. Much of the highly sensitive electronic equipment installed aboard today's war fighting ships are free standing with isolation mounts only on the deck. There is essentially no shock protection for this equipment when subjected to athwartship motion. The intent of this study is to validate the research being conducted at NPS in ship shock modeling by improving the athwartship motion simulations.

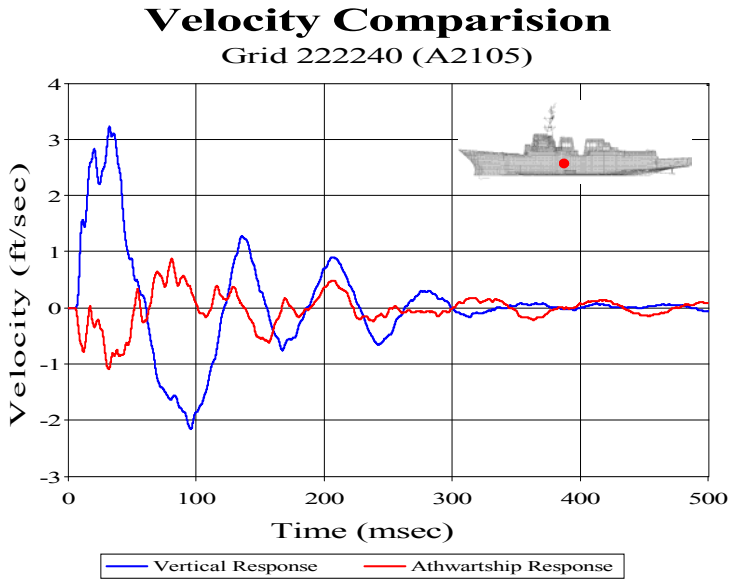

Figure 8. Comparison Between Vertical and Athwartship Velocity Response

A. DRIFT

Measuring the athwartship motion during the ship shock trials on DDG-81 triaxial accelerometers were utilized. These sensors capture and store the acceleration digitally in unit's of gravity. However, all of the time history comparisons presented are velocity vs. time. Due to that fact, all of the sensor data provided by NAVSEA [Ref.11] needed to be integrated and scaled appropriately. Drift occurring in the vast majority of the vertical response integrated data was reported by Schneider [Ref. 4]. This is because the sensor is sampling a frequency range greater than it was intended for. When the acceleration time

history data is integrated the zero position of the velocity curve shifts away from equilibrium. To be certain that the numerical integration routine being used was stable and was not the root source of the drift, several different and more robust integration algorithms were utilized, all with the same results.

Drift compensation has been incorporated into a post processing software tool, UERDtools. This routine requires at least 1000 msec of time history data to function. It was shown to be effective for correcting drift in the vertical response case [Ref. 4]. However, the athwartship response time history curves from the ship shock trails have significant amounts of drift. Using the drift compensation routine in UERDtools does not eliminate the drift. However, residual drift still remains in the athwartship time history curves after applying this technique, leaving the simulation comparisons far less precise as the vertical comparisons [Ref. 5].

Developing a more robust method of drift compensation and applying it to the ship shock trial data was required to be able to conduct an in depth analysis of the athwartship motion. After studying many of the ship shock trial velocity curves it was apparent that the drift resembled second and third degree polynomial curves. By subtracting a second or third degree curve from the time history plot would remove the drift. Using linear algebra algorithm in MATLAB that solves for a polynomial curve of best fit of the original data, and then calculating the difference between the original data and the fitted curve a drift compensated curve would be computed. This method in its simplest form described above is quite powerful, therefore the user must observe caution since it does change the data. Recent upgrades to UERDtools have included a polynomial drift compensation function, however it requires the specification of a start time in which the correction begins. Having to specify a start time for correction requires judgment that may leave too much room for poor engineering practice. Utilizing the linear algebra routine developed in MATLAB requires no judgment since all of the data is used in the curve fitting process. A compromise can easily me achieved by using the UERDtools polynomial drift compensation function applied to all of the data. This method produces the same results as the MATLAB function if and only if the time history curves begins at zero msecs. Appendix C includes a detailed description of the linear algebra routine and a complete program listing. The following figure shows a

comparison between the two drift compensation methods compared with the original sensor data.

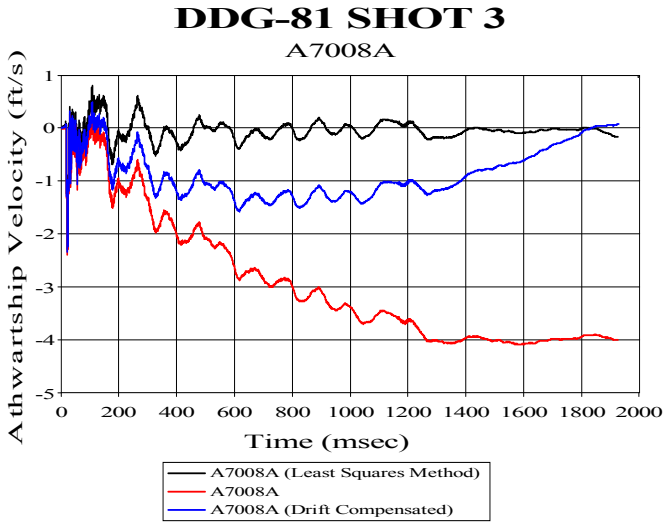

Figure 9. Drift Compensation Methods

B. NOISE

High frequency noise tends to clutter the time history curves of the ship shock trial data. Frequencies above 250 Hz have little to no effect to the overall motion of the ship. Applying low pass filters (filtering all data above 250 Hz) to both of the simulated data and to the ship shock trial data have been performed at NPS throughout recent studies and have been shown to greatly improve data correlation of the mean, variance and standard deviations [Ref. 4]. Figures 10 and 11 shows low pass filtering applied to a set of simulation data. Note that the shape of the curve is not changed as the filter is applied. Filtering in this study has shown to remove the small oscillations from both the shock trial data and the simulation data allowing for greater reliability when comparing curves. Without filtering, there is a band of noise that surrounds the curves making statistical comparisons between the various sensors and nodes difficult to reproduce.

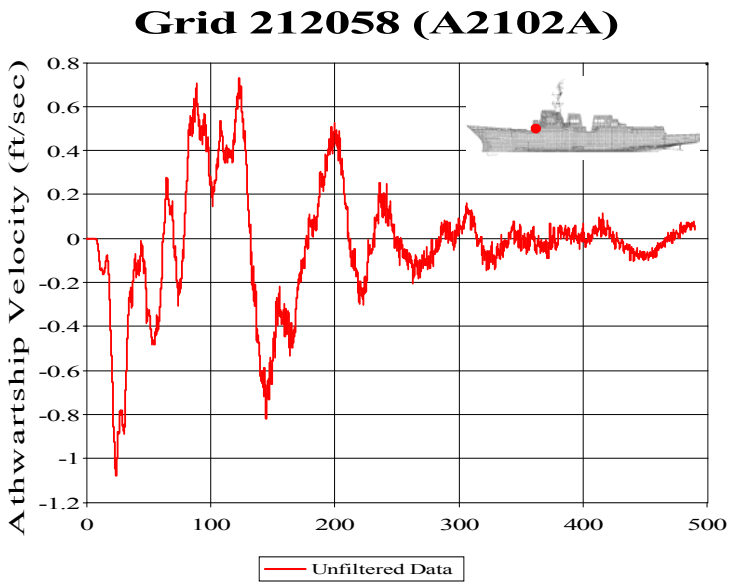

Figure 10. Unfiltered Simulation Data

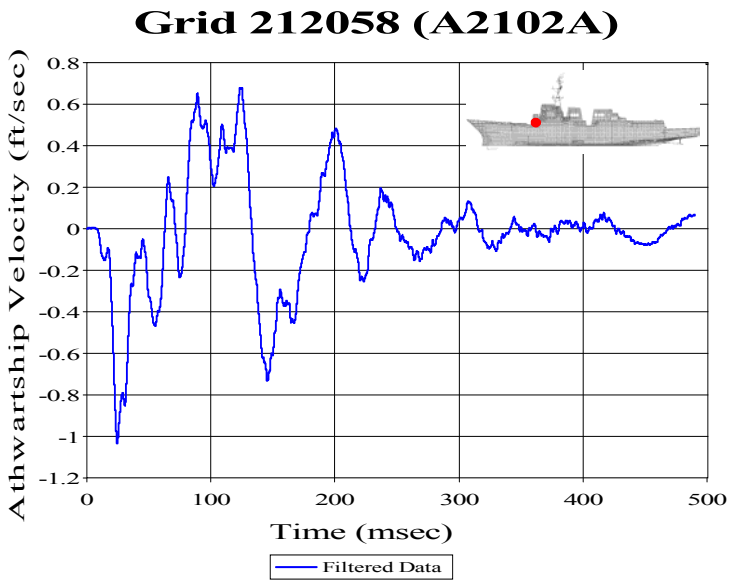

Figure 11. Filtered Simulation Data (250 Hz – Low Pass Filter)

C. ERROR MEASUREMENT

Russell's Error Factor [Ref. 15] was used in the previous DDG-81 studies at NPS and was very effective in characterizing the vertical response. This statistical formula compares differences in magnitude and differences in phase as two separate functions. A comprehensive error factor is developed from the square root of the sum of the squares of the two calculations. From this comprehensive error factor, there are three categories that transient data may be categorized as: Excellent, Acceptable, and Poor. However, recent research in the athwartship motion left some doubt about Russell's Error Factor. Since there were no nodes that were characterized as excellent in Didoszak's study [Ref. 5] perhaps the three categories do not accurately depict the data presented.

The magnitudes of the athwartship motion are three to four times less than their vertical counterparts, yet the simulations are not as nearly as precise according to the same statistical criteria. Looking more closely at the combined time history plots and evaluating the Russell's error factor it can easily be seen that the magnitude error is very low, yet as the time increases over 150 msecs the phase between the two curves seems to vary. The general trend of the curve is modeled quite well, yet it appears to be out of phase as time increases to 500 msecs. Figures 12 through 14 depict this trend common to the majority of the athwartship simulations.

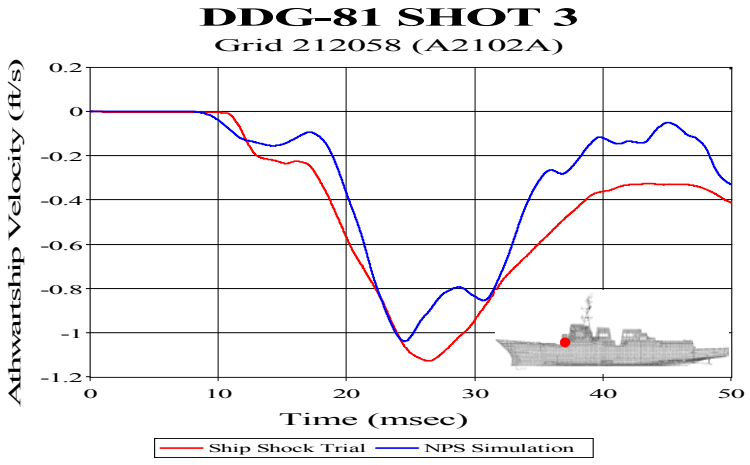

Figure 12. 50 msec Comparison

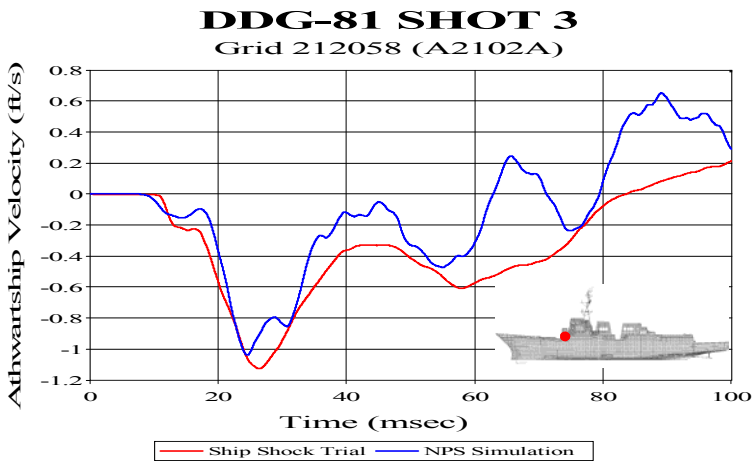

Figure 13. 100 msec Comparison

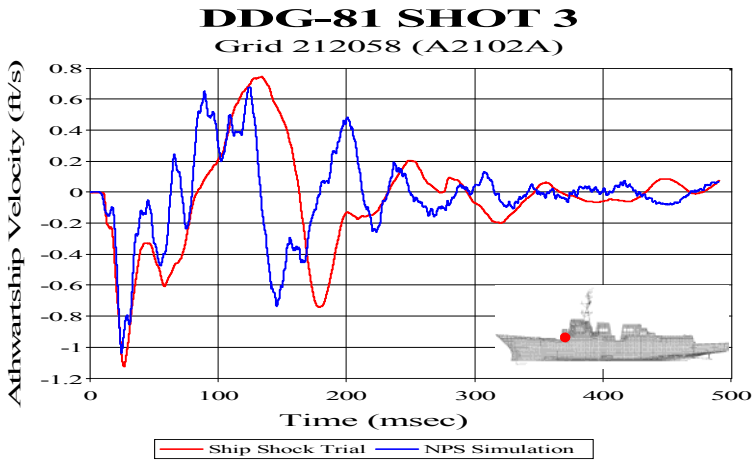

Figure 14. Full 500 msec Comparison

Russell's error changes dramatically as time increases throughout the simulation. Table 2 shows the relatively low and consistent magnitude errors. The phase error however, which is extremely low in the early time history, grows beyond the acceptable range. The phase error seems to be the greatest obstacle to overcome in the athwartship simulations. All error comparisons previously conducted at NPS were performed with 500 msec time history curves.

Grid 212058 (A2102A)	Magnitude Error (RM)	Phase Error (RP)	Comprehensive Error (RC)
Figure 12 – 50 msec	0.15	0.07	0.15
Figure 13 – 100 msec	0.10	0.21	0.21
Figure 14 – 500 msec	0.14	0.38	0.36

Table 2. Russell's Error Factor Comparison as Time Increases

THIS PAGE INTENTIONALLY LEFT BLANK

IV. INTRODUCTION TO THE SHOCK SPECTRA

Previous studies conducted at NPS have concentrated solely on time history analysis and efforts to validate the computer modeling effort. Introducing shock spectra analysis shows the data comparison between computer simulations and shock trials in the frequency domain. This allows for various aspects of UNDEX and simulations to be compared that aren't easily recognizable in the time domain.

A. SHOCK SPECTRA BACKGROUND

The shock spectra is defined as the maximum absolute response of an undamped single degree of freedom system produced by a shock loading [Ref. 9]. If one were to calculate the response of a system at a certain frequency a curve would be generated. Using iterative programming the response of a system can be characterized by a series of curves, each curve representing the response for a unique frequency. Instead of analyzing many different curves, it is convenient to view the maximum absolute value from each frequency. These maximum values plotted on one curve form the shock spectra. Time history plots can be used to generate shock spectra plots with a simple algorithm. UERDtools has a very useful shock spectra generating function that enables quick generation of these spectra plots in a variety of formats including triaxial plots.

Since there is no phase in a shock spectra plot, the phase concerns described in the previous chapter are eliminated. Also, being able to pay particular attention to certain frequencies shows unlimited potential for future design of shock isolation mounts and systems. As another method of validating the use of computer models for naval ship shock trials there seems to be more practical uses involved with the shock spectra analysis than with the time history analysis.

B. EVALUATING THE SHOCK SPECTRA

The following figure is an example of a shock spectra plot and its corresponding time history plot including curves from shot 1 of the DDG-81 ship shock trial and the NPS computer simulation of the same.

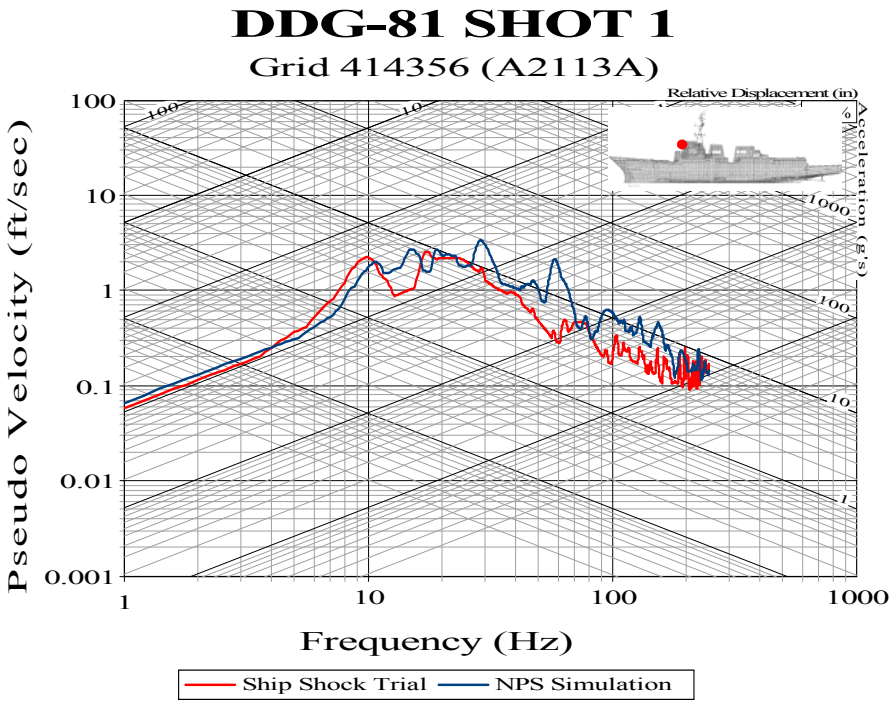

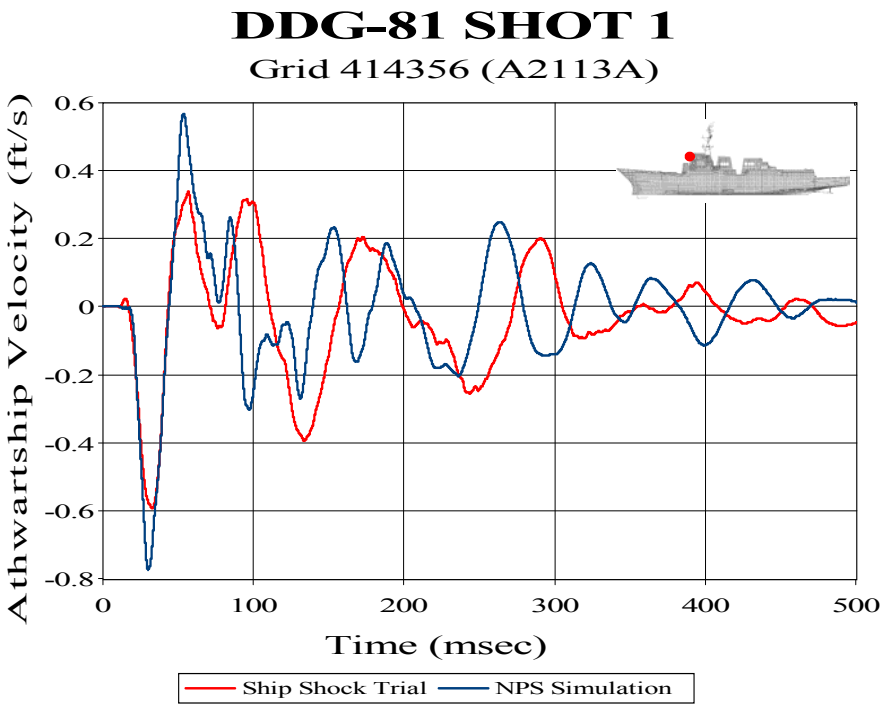

Figure 15. Sample Shock Spectra Plot (top) and Corresponding Time History (bottom)

Analyzing the amount of data presented in this plot may be somewhat overwhelming at first, but essentially it is very easy to understand. First, the x and y axes are both logarithmic. The y-axis is labeled "Pseudo Velocity," due to the fact that the peak response occurs after the event (UNDEX in this particular case). Being in the frequency domain vice the time domain it is easy to compare the response at specific frequencies, most importantly the lower natural frequencies of the structure. The diagonal and off-diagonal axes also provide the relative displacement and acceleration. For example, to read the acceleration response at a certain frequency we would identify the point at which the curve intersects that particular frequency, then follow the diagonal axis down and to the right of the plot. Likewise, for reading the relative displacement response at that same frequency we would again start at the intersection of the curve at that particular frequency, then follow the off-diagonal axis up and to the right of the plot. The top and right sides of the plot include values for the displacement and acceleration in logarithmic form.

Below 10 Hz the simulation data and the actual data curves are nearly on top of each other. The low frequency data in the shock spectra plot originates from the early time response. In this case the early time response of the simulation is very accurate as shown in corresponding time history plot.

Between 10 Hz and 100 Hz there are some fluctuations between the two curves and above 100 Hz there is an even higher degree of fluctuation. It is essential to recognize that this is a logarithmic plot and approx two-thirds of all of the data presented is below 1 ft/sec. For example, there appears to be a gap between the simulation and actual data at 100 Hz, however there is only 0.3 ft/sec difference between the two curves. When compared to the peak response of the vertical motion, 0.3 ft/sec may be considered negligible. Without using the log scale, the two curves would essentially be blurred together and reading information from the plots would be difficult. Yet, the log scale does prove without any doubt that the simulation effectively models the low frequency response of the UNDEX attack extremely well.

THIS PAGE INTENTIONALLY LEFT BLANK

V. EVALUATION AND ANALYSIS

A. TIME HISTORY ANALYSIS

Each time history from the ship shock trial athwartship data used in the DDG-81 comparison had significant drift. As described in Chapter III, polynomial curve fitting was utilized to remove this drift. In previous studies Russell's Error Factor has been used to benchmark the level of accuracy in the NPS simulations. An analysis conducted an of the athwartship response and concluded that the drift associated with the sensor data from the actual ship shock trial overwhelmed the rather small magnitudes computed in the simulation [Ref. 5.]. Also noted in the study was that the late time phase error in combination with the significant drift resulted in poor data correlation using the Russell's error criteria.

Figure 17, is an athwartship response comparison of Russell's Error Factor from a previous study [Ref. 5]. All of the data compiled in this figure was taken from 500 msec time history plots. Figure 18 shows the Russell's Error Factor comparisons from shot 1 in this study. The pink squares depict the Russell's Error, both phase and magnitude for the 100 msec time history. It is clear from the figures that there is a marked improvement in study presented in this paper due to the reduction of the phase error. More than half of points have a magnitude error of less than 0.1 that can most likely be attributed to the polynomial drift compensation technique.

The vast majority of the phase error is from the last half of the time history. Although, the magnitude of the response may be accurately simulated the curves are often completely out of phase after the first 250 msecs. It is in this late time portion of time history that the response is typically less than 0.2 ft/sec. The peak response in is captured in the first 70-80 msecs in the three shots analyzed, and the simulations have performed exceptionally well in modeling the early time response. Yet, according to the Russell's Error Factor guidelines the phase and magnitudes errors are weighed equally in determining the comprehensive error. Because it seems that the negligible late time athwartship motion is adversely affecting the integrity of the simulation efforts a similar

comparison was performed using just the first 100 msecs. The comparison made with the 100 msec time history is much better than the 500 msec comparison.

Similar Results were noticed in the analysis of shot 2 as shown in Figure 19 and Shot 3 as shown in Figure 20. Shot 2 has historically been the least accurate athwartship simulation based on Russell's Error Factor comparisons [Ref. 5]. However, when evaluating just the first 100 msecs the data correlates well with two comparisons in the excellent range and the majority in the acceptable range.

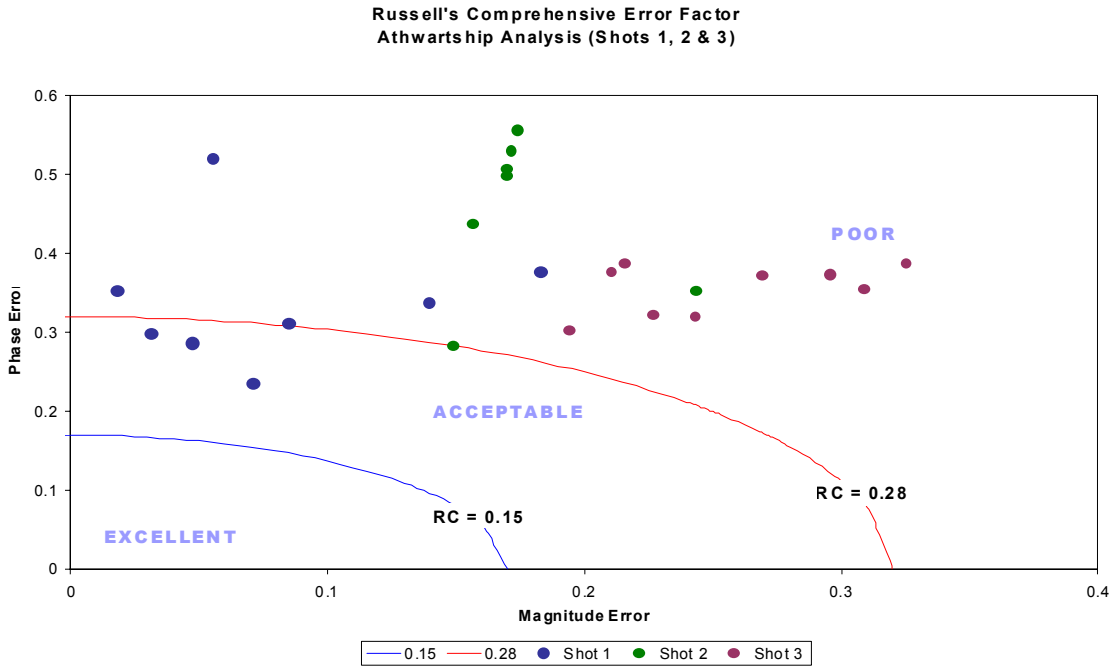

Figure 16. Russell's Error Factor Comparison from Previous Study [From Ref. 5]

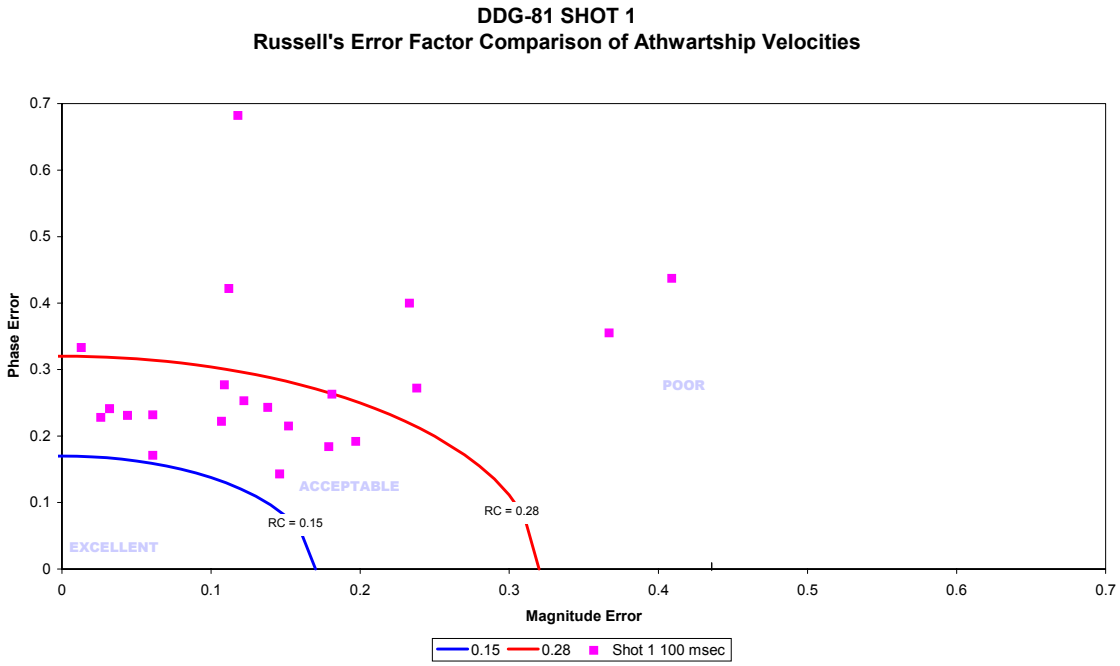

Figure 17. Russell's Error Factor Comparison for Shot 1

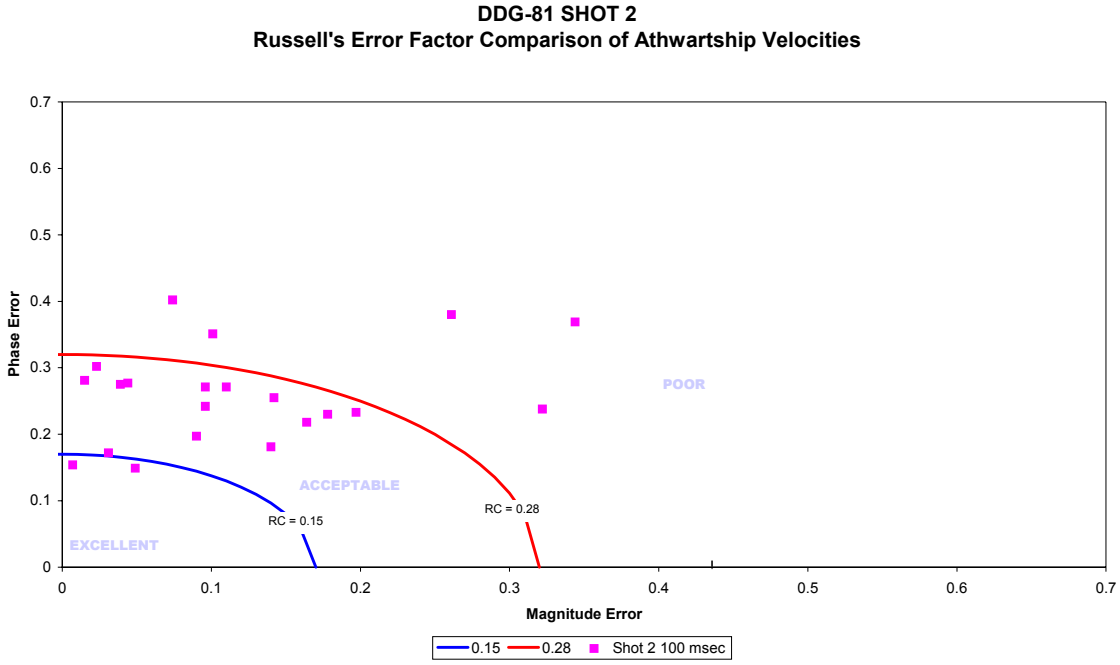

Figure 18. Russell's Error Factor Comparison for Shot 2

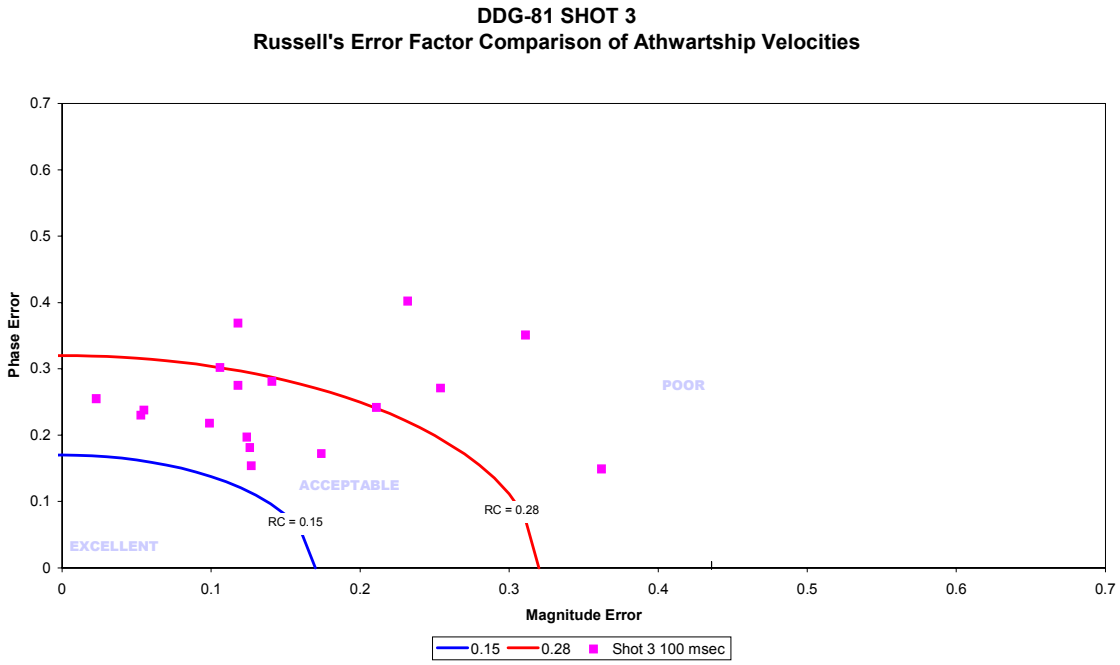

Figure 19. Russell's Error Factor Comparison for Shot 3

Outliers within the shock trial data have been previously identified at NPS [Ref. 4]. Having evaluated a different set of sensors and nodes in this study specific bow and stern sensors identified in the past were avoided. However, when comparing the nodal response from the simulations there were a few instances in which the actual sensor data seemed corrupt. For example, Figure 20 shows one of these outliers. In every case evaluate the peak response occurred within the first 100 msecs. However, this sensor data has captured a peak response of –6 ft/sec at approximately 350 msecs. The amplitude of the peak response of this sensor raises doubts as to its accuracy. Compared with hundreds of other athwartship response plots, this sensor's response does not seem to dampen. This sensor when compared to simulation results had a high Russell's Error Factor in all three shots.

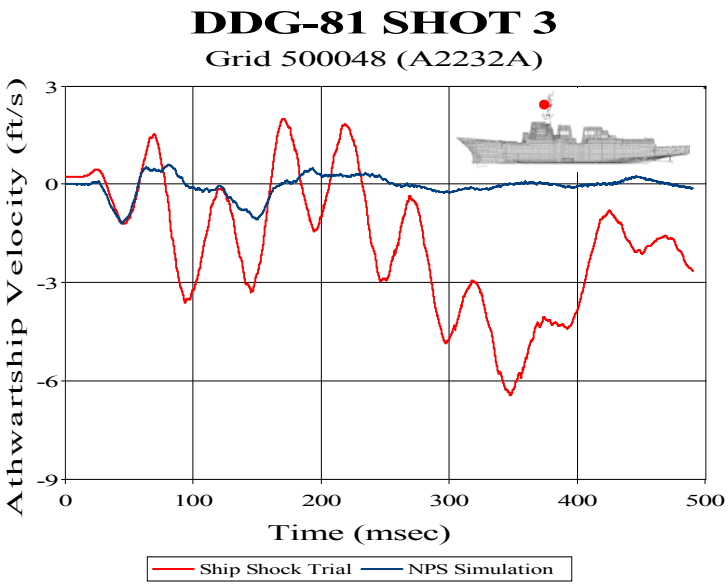

Figure 20. Example of Outlier

B. SHOCK SPECTRA ANALYSIS

As described earlier there is no phase in a shock spectra plot. Therefore the concerns with late time phasing between the simulation and the actual trial data have been eliminated. Evaluating the data in the frequency domain allows for a different perspective on the physical behavior of the UNDEX attack and the simulation. As seen from various time history plots, the magnitudes of the athwartship motion are small in comparison to the magnitudes of the vertical motion. This fact is also depicted in the shock spectra plots. The majority of all the data presented in the athwartship shock spectra plots is below 1 ft/sec in velocity. Some of the peak values shown in this study are between 2 and 3 ft/sec and can be compared to a gentle swell in the ocean.

NPS simulations have performed exceptionally well in the 1 to 10 Hz range, there is little difference between the two curves in this range. The majority of these plots shown in Appendix B. display a gradual rise in amplitude as the frequency increases. Between 10 and 50 Hz the peak response has occurred and there is a downward trend. However, there tends to be some spikes between 10 and 20 Hz. Above 50 Hz the response fluctuates a great deal but the downward trend is prevailing. It can be shown

that the NPS simulations over predict the high frequency responses from approximately 70 Hz upwards. These values all fall below 1 ft/sec, and on the log scale the curves still remain close. The upper limit for all of these shock spectra plots was set at 250 Hz since the data was low-pass filtered. The following table is a general summary of the Shock Spectra analysis by frequency range.

Frequency	Trend	Shot 1	Shot 2	Shot 3
1 to 10 Hz	Gradual rise to peak value (approx. 3 ft/sec)	Simulation closely matches trial data	Simulation closely matches trial data	Simulation routinely under predicts trial data
10 to 30 Hz	Oscillation near peak values (within 1 to 2 ft/sec)	Simulation closely matches or slightly over predicts trial data	Simulation closely matches or slightly over predicts trial data	Simulation leads trials data by 5 Hz
30 to 70 Hz	Consistent response below peak	Simulation closely matches or slightly over predicts trial data	Simulation routinely over predicts trial data	Simulation routinely over predicts trial data
70 to 100 Hz	Peak value occurs (approx. 3 ft/sec) then sharp decline	Simulation routinely over predicts trial data	Simulation routinely over predicts trial data	Simulation routinely over predicts trial data
100 to 250 Hz	High degree of oscillation (below 1 ft/sec)	Simulation closely matches or slightly over predicts trial data	Simulation closely matches or slightly over predicts trial data	Simulation closely matches or slightly over predicts trial data

Table 3. Summary of Shock Spectra Analysis of Shots 1, 2 and 3

C. NUMERICAL EVALUATION OF DATA

Throughout the course of this study great attention has been paid to concepts such as drift and late time phase disparities. The sensors used in the DDG-81 ship shock trial were 12-bit sensors calibrated to record data between –200g and 200g. This range has adequately recorded the vertical motion yet 12 bit technology handles 2^{12} (4096) possible values. Therefore, the step size is fixed with a resolution 0.098g which is calculated by dividing the calibration span by the step size. In other words, the sensor is limited in its ability to accurately capture the high frequency, low amplitude response that is typical of the athwartship motion [Ref. 16]. Reducing the span that the sensors are calibrated to a lower value would increase the resolution of the late time response. This would also be very impractical since the vertical response would essentially be chopped.

For example, if 16 bit sensors were utilized instead of 12 bit sensors during the ship shock trial the amount steps available for recording would be 2^{16} (65536). Therefore the resolution would be 0.0061g using the same calibration span. Both the vertical and athwartship responses could be accurately recorded and the amount of drift shown in the late time response would be reduced or even eliminated. However, high frequency noise filtering may become even more important when processing data since the ability to capture this range is improved by an order of magnitude.

THIS PAGE INTENTIONALLY LEFT BLANK

VI. CONCLUSIONS AND RECOMMENDATIONS

A. SUMMARY OF FINDINGS

Although very low in magnitude when compared to the vertical response, the athwartship response remains an important aspect of an UNDEX attack. Being able to accurately predict the athwartship response serves as a means validate this technique. This thesis has focused on the reasons why past simulations have yet to model the athwartship response with the degree of accuracy as the vertical response and ways to improve the simulation results.

The largest obstacle in modeling the athwartship response is the reliability of actual ship shock trial data. 12 bit sensors used in the trials have not adequately recorded the late time response leaving significant amounts of drift in the integrated velocity data. Reducing this drift has been the key to improving the accuracy of the simulations. Russell's Error Factor is a technique used to compare two sets of data. However, if a set of actual trial data is corrupt the simulation data will correspond poorly. In other words, the simulation may be accurate, but the error will be high. Looking beyond statistical error is essential when evaluating the differences between the simulation and trial data.

Using more strict criteria in the selection of nodes has been shown to modestly improve the simulation results. These improvements have not been nearly as substantial as those shown by compensating the drift with polynomial curve fitting. However, selecting the node that best represents the location of a sensor is always desirable.

Shock spectra analysis can serve as a design tool as well as a tool for comparative analysis. Barge testing has been used to shock qualify naval equipment for years, yet using these UNDEX simulations and the shock spectra's created accurate predictions of the frequency response can be achieved. As a comparative tool, the shock spectra has shown that the low frequency response is very accurately modeled, and in many cases the simulation are more conservative than the actual trial data.

Determining the amount of data required to perform the analysis of the athwartship motion is essential. Unlike the vertical response, 500 msec time histories of the athwartship response may be too much information. When evaluating just the first

100 msecs the peak response is captured and has been simulated to the level of accuracy of previous vertical response studies. The late time response is so low in magnitude that it may be considered negligible. Gentle sea swells greatly exceed the average late time response. Clearly, a response that low in magnitude is not going to be a concern of any surface ship commander, naval architect, marine engineer, or anyone else involved the UNDEX community.

B. FUTURE WORK

Being able to analyze different types of UNDEX attacks are of great interest to the military. This thesis along with previous studies conducted at NPS has served to benchmark the validity of using simulations instead of live fire shock testing. In light of recent events including the USS Cole suicide attack (2000), and the USS Samuel B. Roberts mine explosion (1988) the ability to simulate hull damage due to close in explosions may have the potential to save lives. The whipping effects due to the gas bubble oscillation have been blamed for sinking many liberty ships in WWII. This is another area that modeling may serve to improve hull design.

Using the same techniques described in this thesis, the UNDEX simulation of a ship while still in the design phase may be the next step. More specifically, the next generation destroyer (DDX) can be modeled in the same fashion that DDG-81 was modeled. Environmental regulations are only going to become more strict, and the day may come that live fire ship shock testing will be outlawed. These simulations may serve as the only way to evaluate the response of a surface ship to and UNDEX attack.

In the near future the application of 16 bit accelerometers as compared to the 12 bit accelerometers that were used in the DDG-81 ship shock trials will increase the resolution of the ship's response. Increased resolution will lead to the elimination of the velocity drift, enabling for more accurate comparisons of these simulations to the trial data.

APPENDIX A. DDG-81 ATHWARTSHIP TIME HISTORY PLOTS

A. SHOT 1

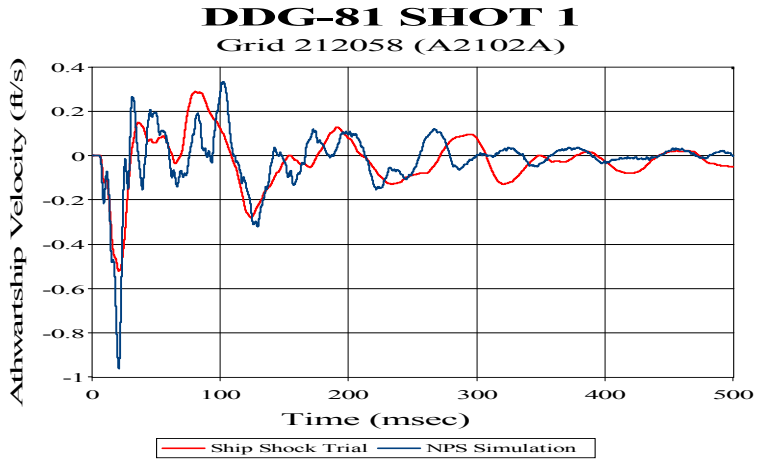

Figure 21. Combat Information Center (1-126-0-C) Deck Sensor FM 126

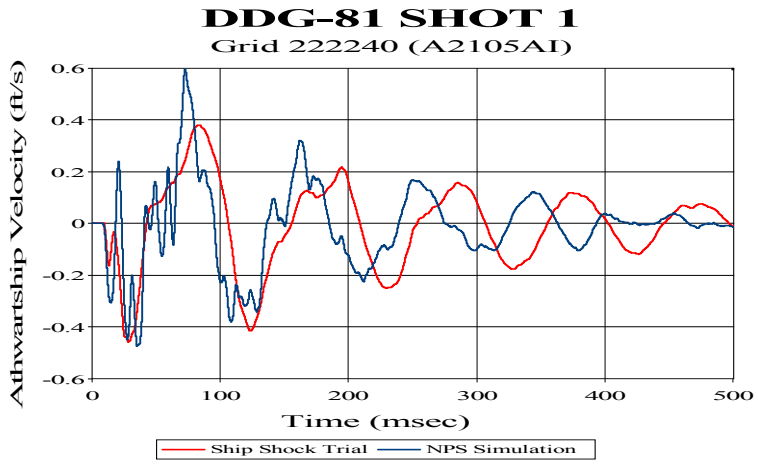

Figure 22. Combat Information Center Annex (1-126-0-C) Deck Sensor FM 174

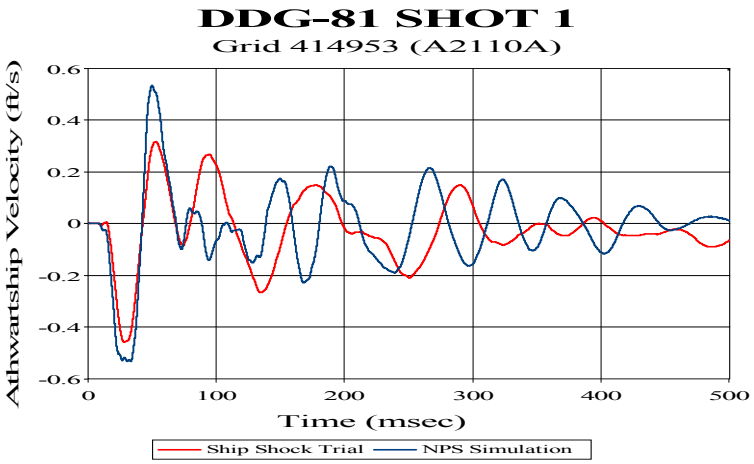

Figure 23. Radar Room #1 (03-128-0-C) Bulkhead Sensor

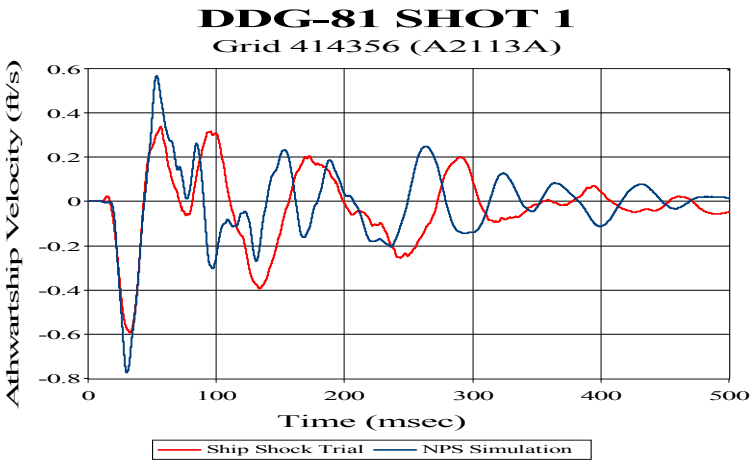

Figure 24. Passage Way (02-133-1-L) Overhead Sensor FM 142

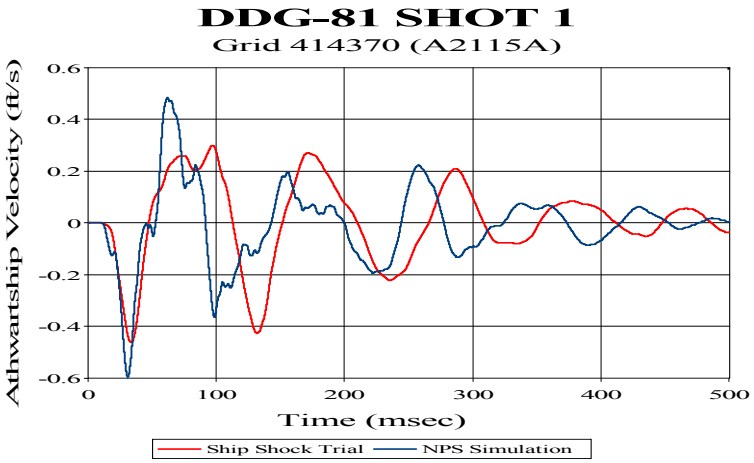

Figure 25. Radar Room #2 (03-142-0-C) Deck Sensor

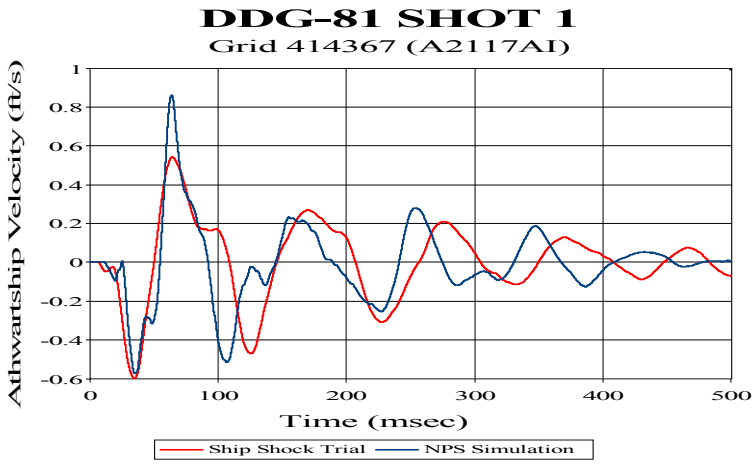

Figure 26. Radar Room #2 (03-142-0-C) Deck Sensor FM 174

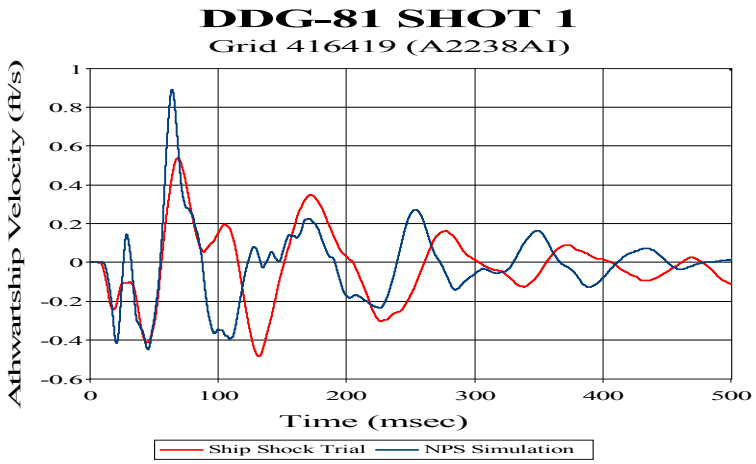

Figure 27. Port Mast Leg (MAST) Forward Outboard Corner

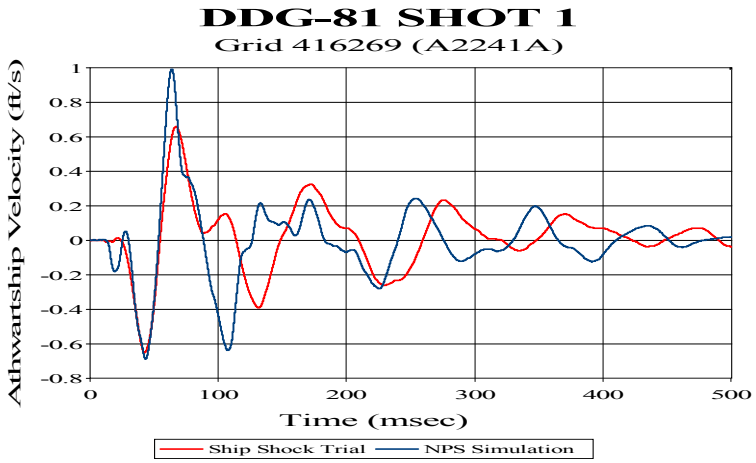

Figure 28. Stbd Mast Leg (MAST) Forward Outboard Corner

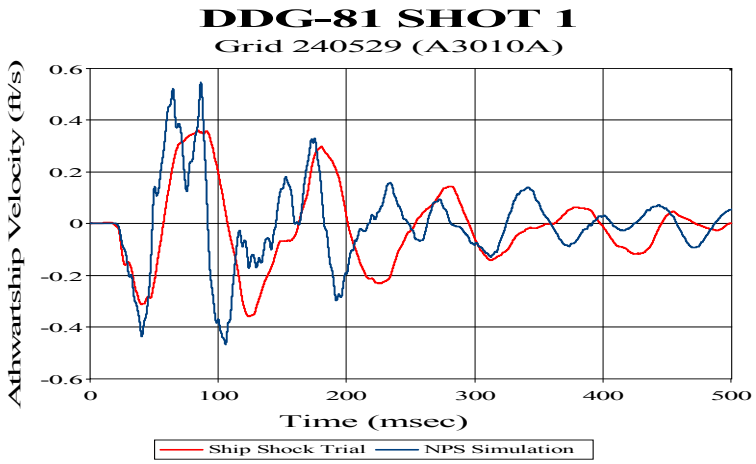

Figure 29. Central Control Station (1-268-0-C) Deck Sensor

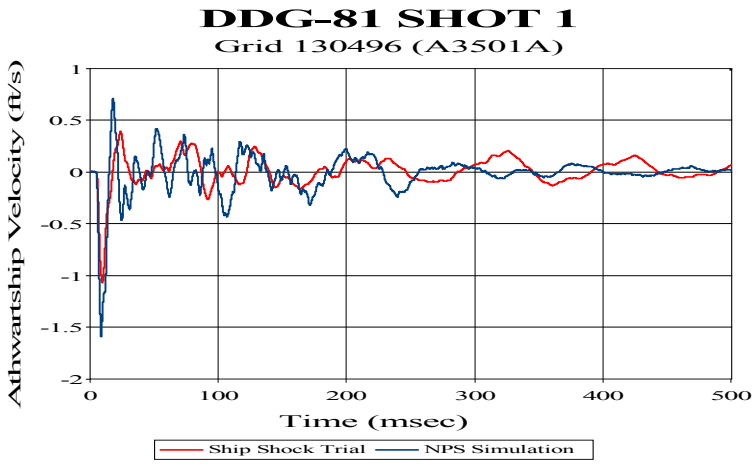

Figure 30. Combat Systems Equipment Room #1 (2-053-1-C) Deck Sensor

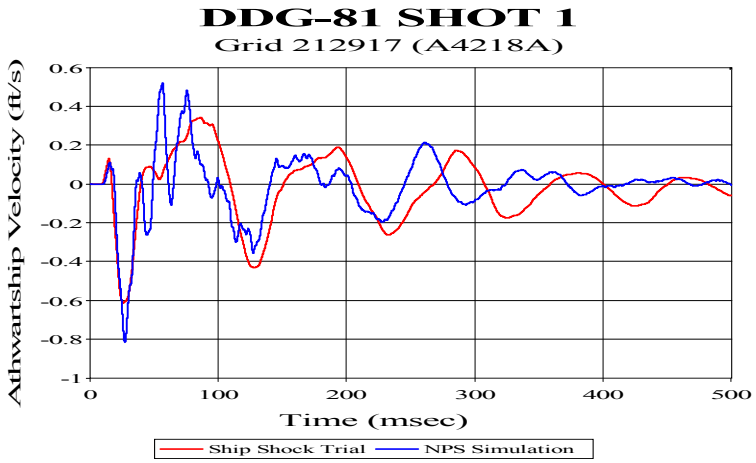

Figure 31. Combat Systems Maintenance Center (01-130-0-Q) Deck Sensor

B. SHOT 2

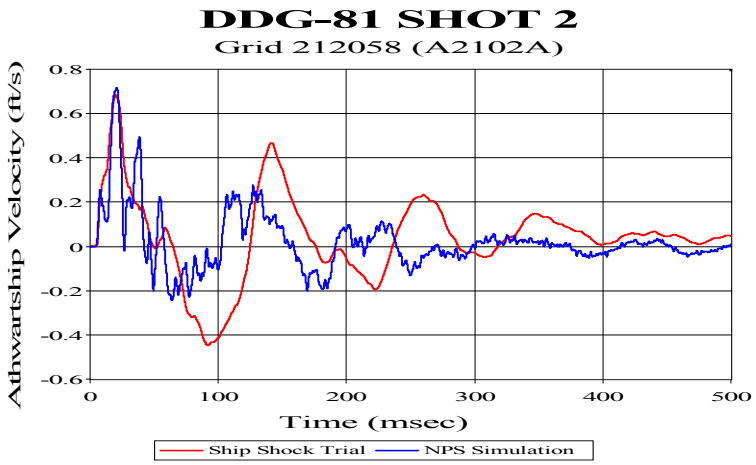

Figure 32. Combat Information Center (1-126-0-C) Deck Sensor FM 126

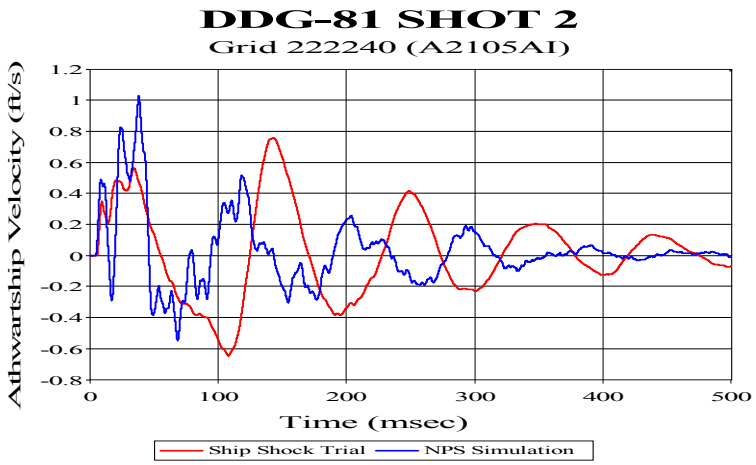

Figure 33. Combat Information Center Annex (1-126-0-C) Deck Sensor FM 174

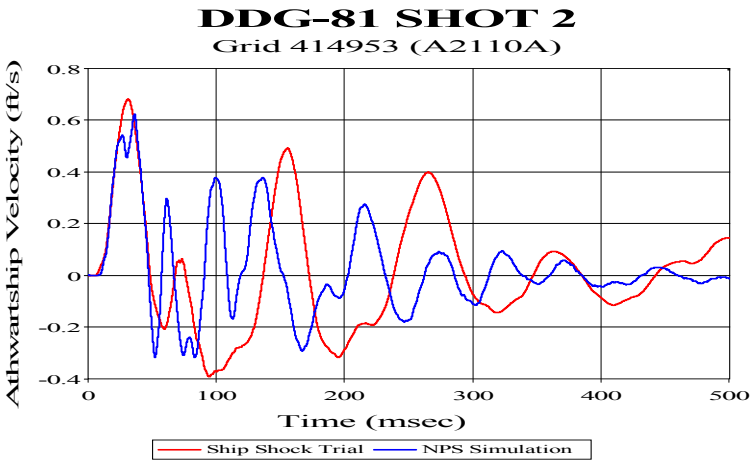

Figure 34. Radar Room #1 (03-128-0-C) Bulkhead Sensor

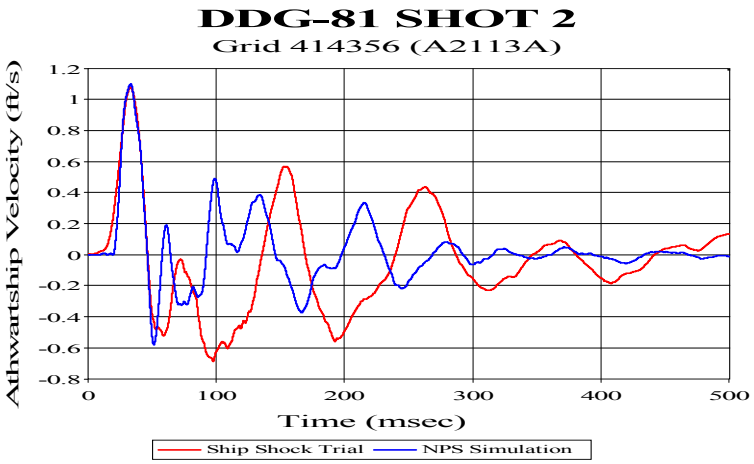

Figure 35. Passage Way (02-133-1-L) Overhead Sensor FM 142

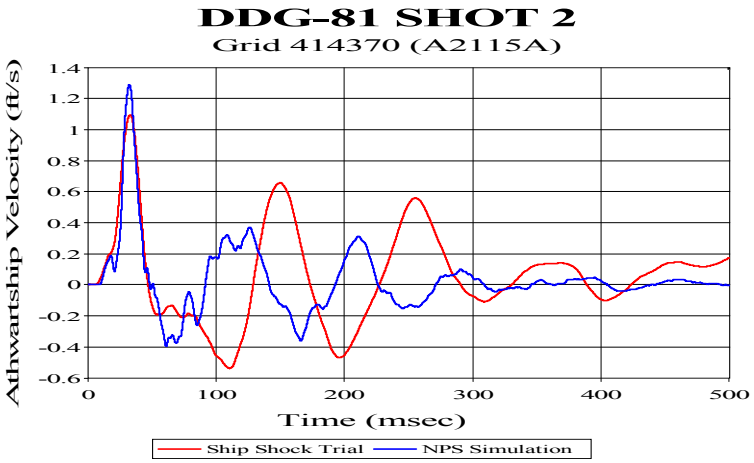

Figure 36. Radar Room #2 (03-142-0-C) Deck Sensor

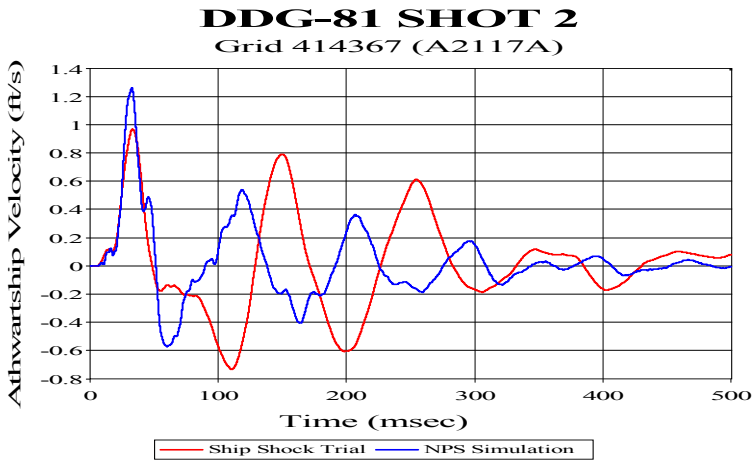

Figure 37. Radar Room #2 (03-142-0-C) Deck Sensor FM 174

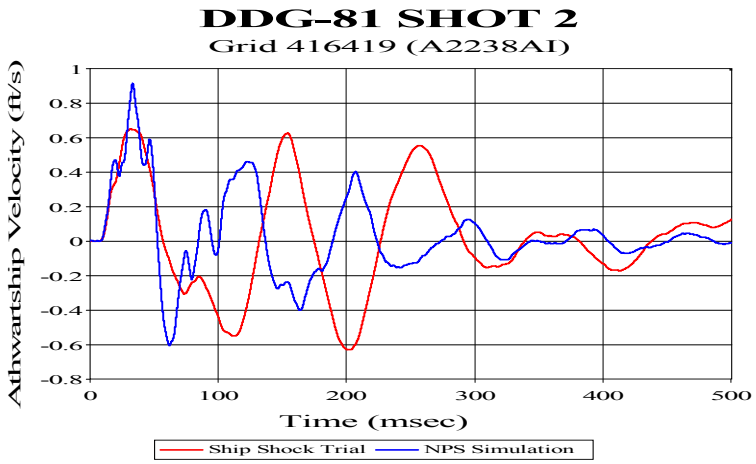

Figure 38. Port Mast Leg (MAST) Forward Outboard Corner

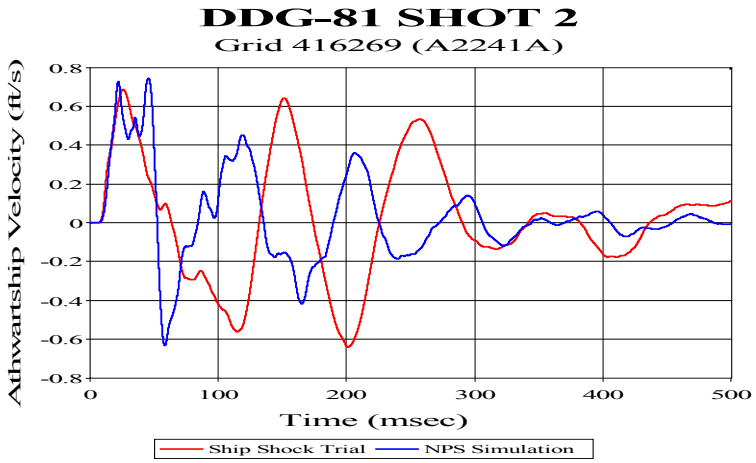

Figure 39. Stbd Mast Leg (MAST) Forward Outboard Corner

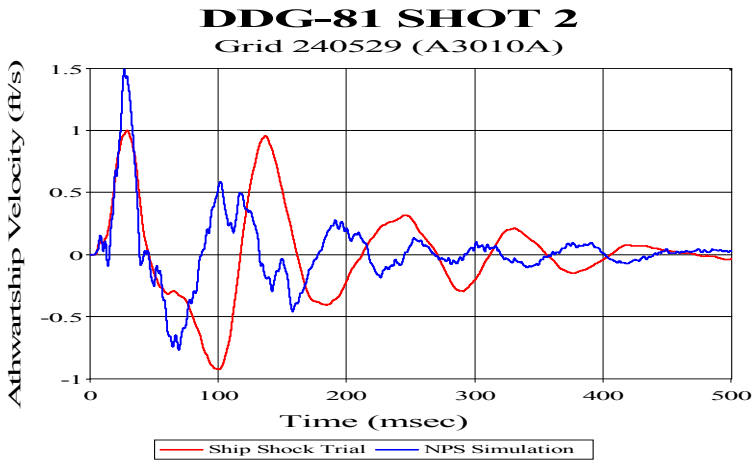

Figure 40. Central Control Station (1-268-0-C) Deck Sensor

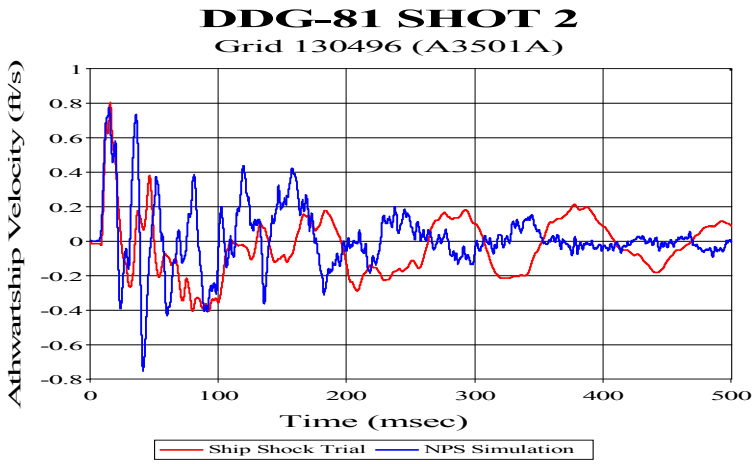

Figure 41. Combat Systems Equipment Room #1 (2-053-1-C) Deck Sensor

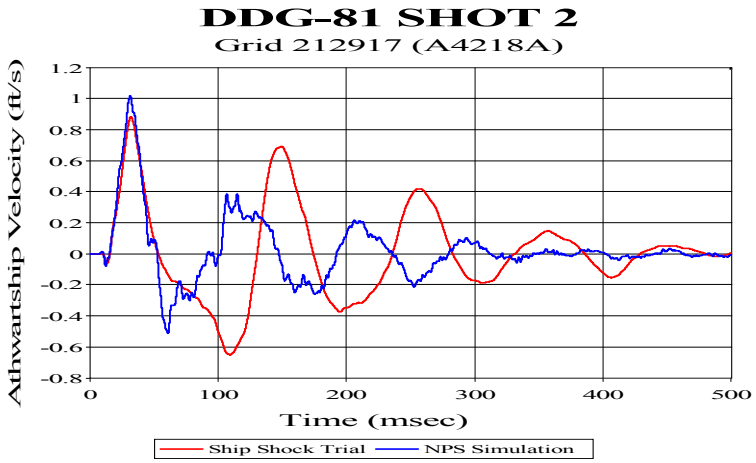

Figure 42. Combat Systems Maintenance Center (01-130-0-Q) Deck Sensor

C. SHOT 3

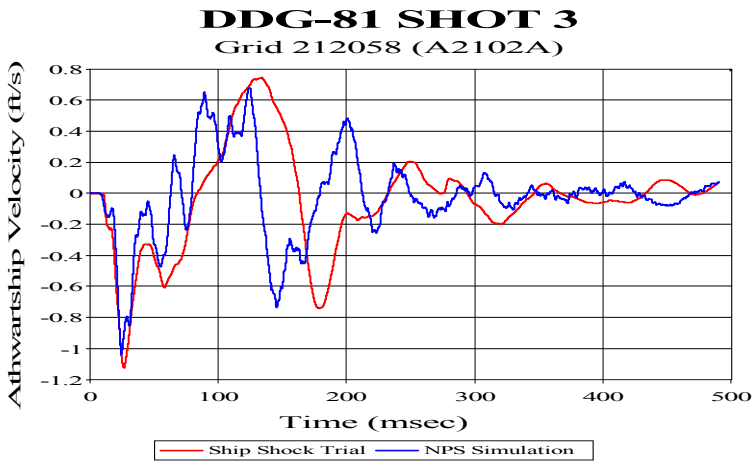

Figure 43. Combat Information Center (1-126-0-C) Deck Sensor FM 126

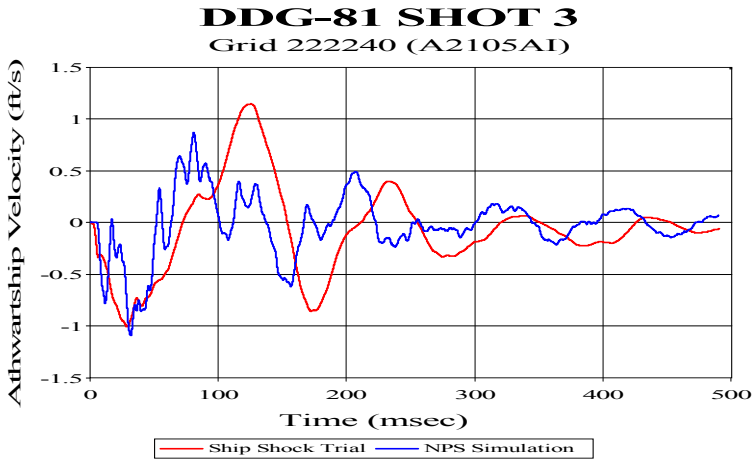

Figure 44. Combat Information Center Annex (1-126-0-C) Deck Sensor FM 174

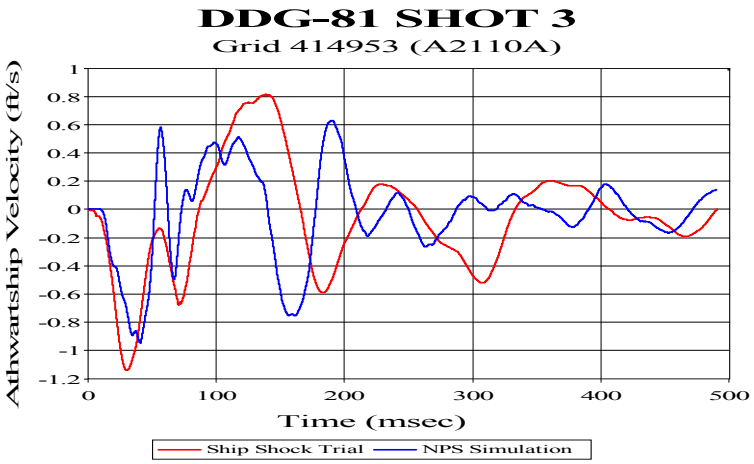

Figure 45. Radar Room #1 (03-128-0-C) Bulkhead Sensor

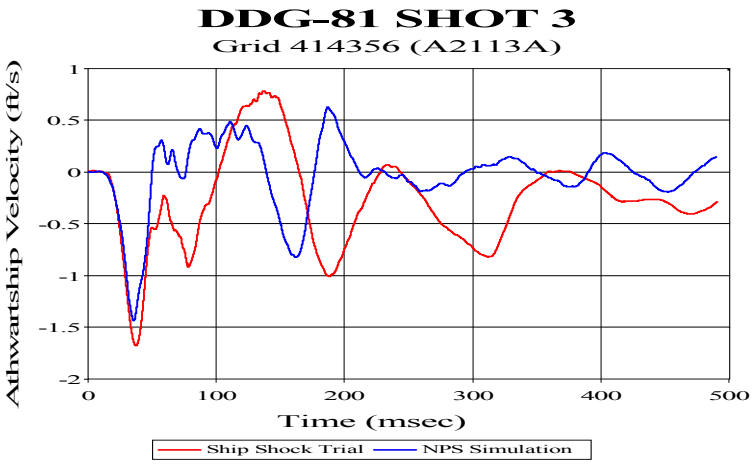

Figure 46. Passage Way (02-133-1-L) Overhead Sensor FM 142

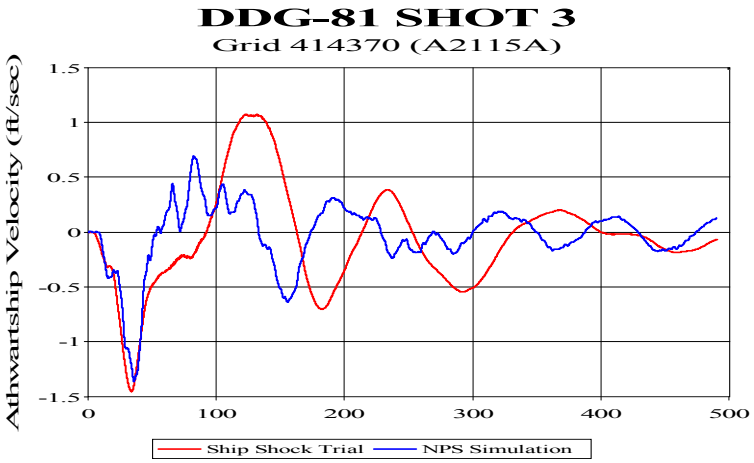

Figure 47. Radar Room #2 (03-142-0-C) Deck Sensor

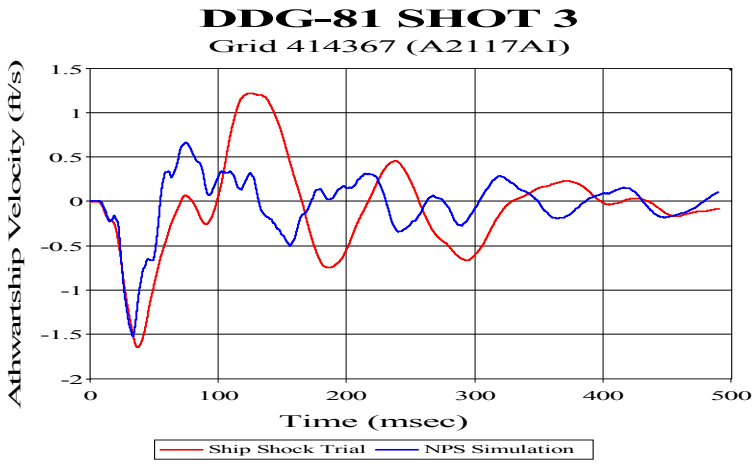

Figure 48. Radar Room #2 (03-142-0-C) Deck Sensor FM 174

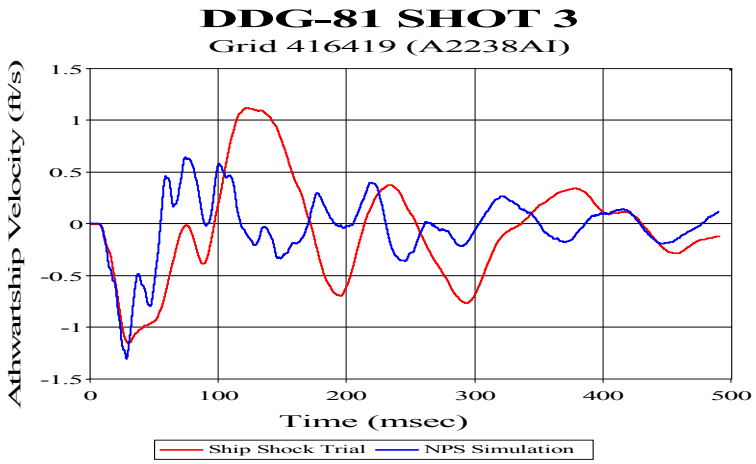

Figure 49. Port Mast Leg (MAST) Forward Outboard Corner

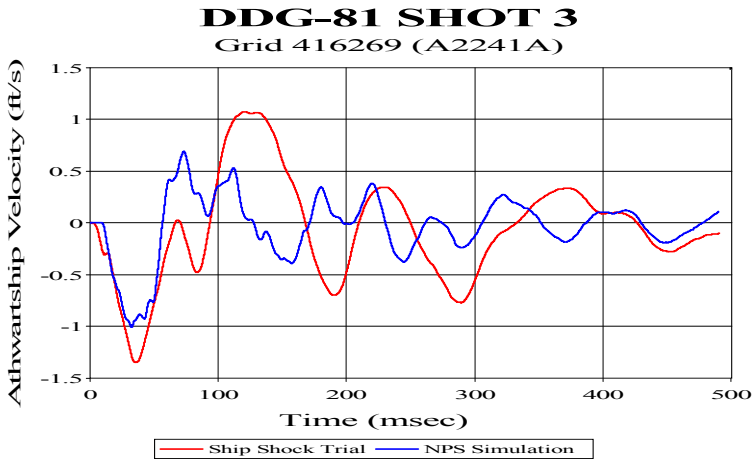

Figure 50. Stbd Mast Leg (MAST) Forward Outboard Corner

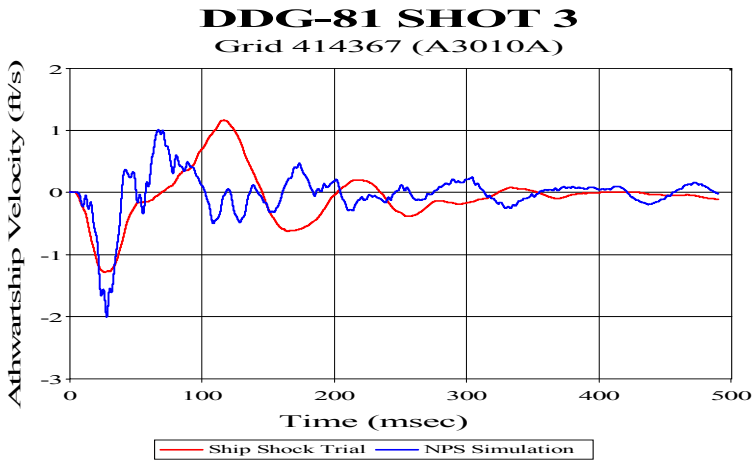

Figure 51. Central Control Station (1-268-0-C) Deck Sensor

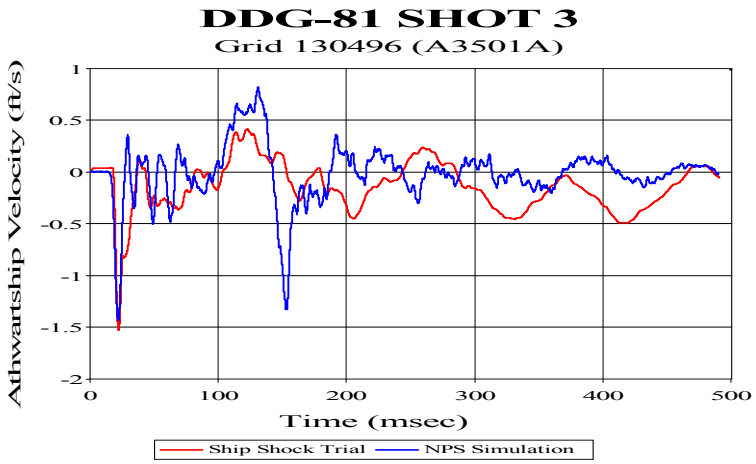

Figure 52. Combat Systems Equipment Room #1 (2-053-1-C) Deck Sensor

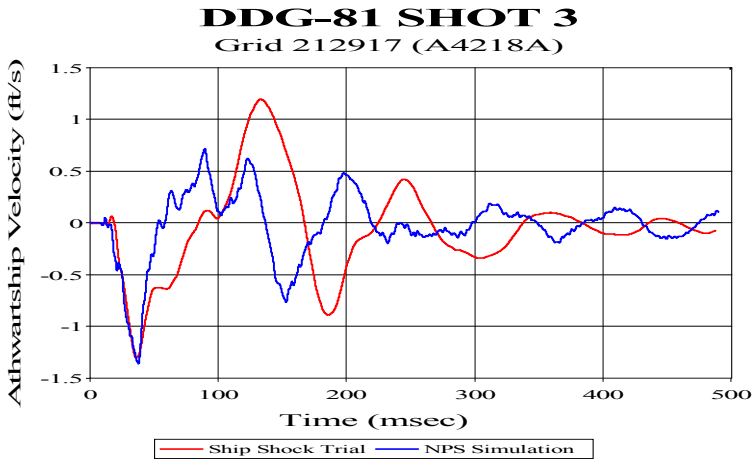

Figure 53. Combat Systems Maintenance Center (01-130-0-Q) Deck Sensor

APPENDIX B. DDG 81 ATHWARTSHIP SHOCK SPECTRA PLOTS

A. SHOT 1

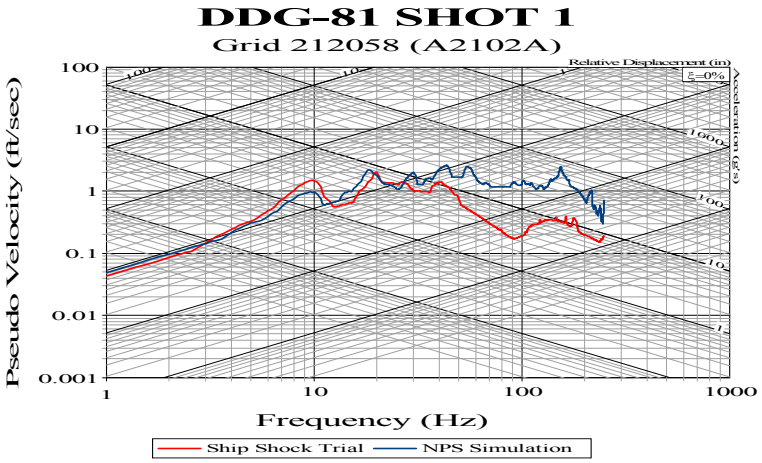

Figure 54. Combat Information Center (1-126-0-C) Deck Sensor FM 126

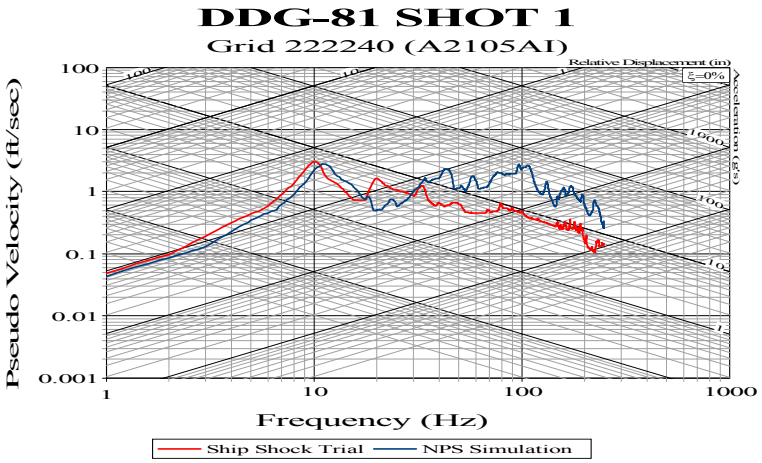

Figure 55. Combat Information Center Annex (1-126-0-C) Deck Sensor FM 174

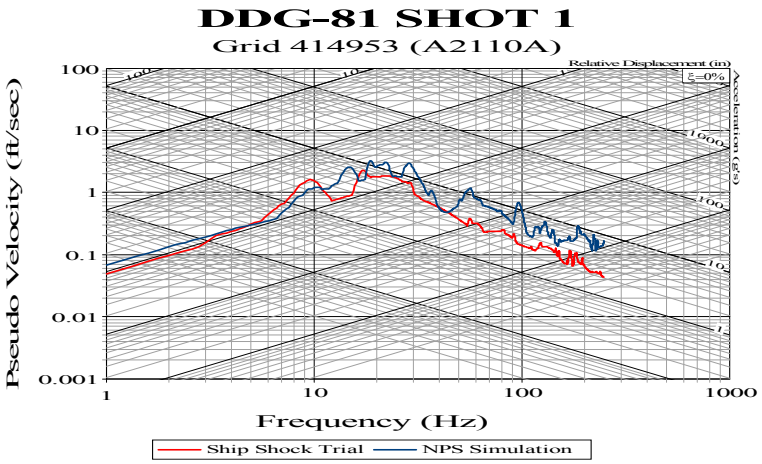

Figure 56. Radar Room #1 (03-128-0-C) Bulkhead Sensor

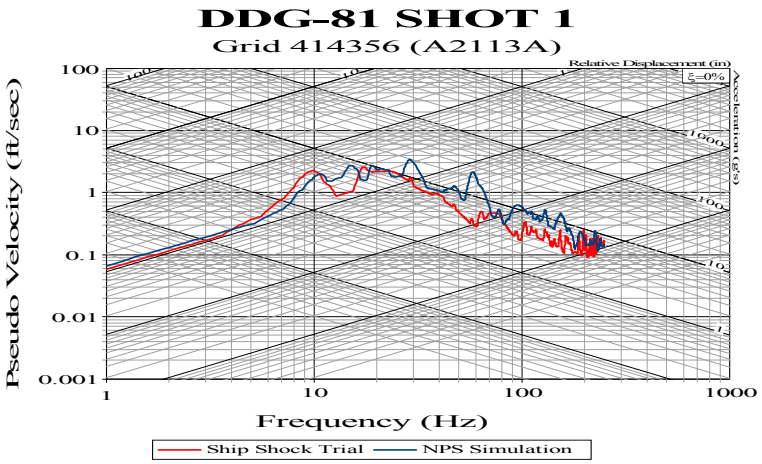

Figure 57. Passage Way (02-133-1-L) Overhead Sensor FM 142

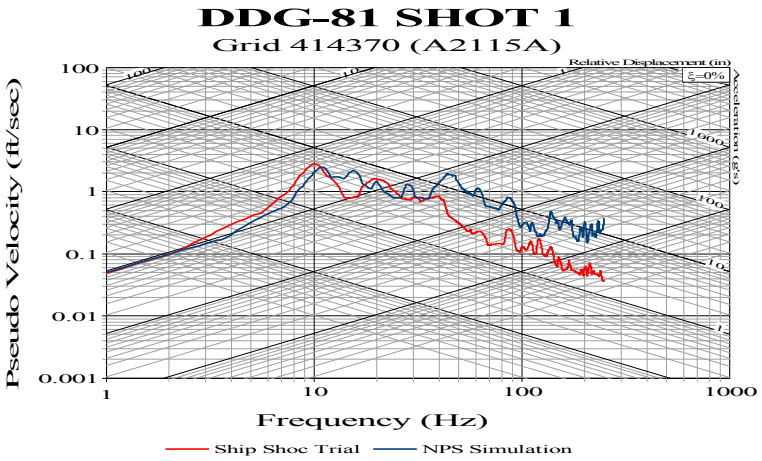

Figure 58. Radar Room #2 (03-142-0-C) Deck Sensor

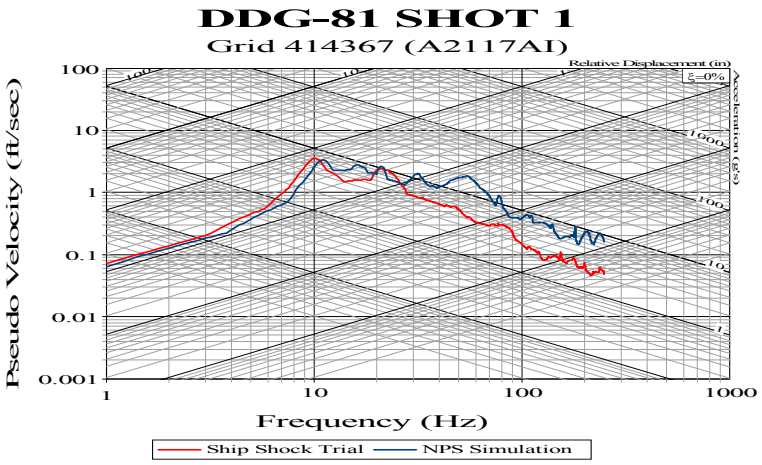

Figure 59. Radar Room #2 (03-142-0-C) Deck Sensor FM 174

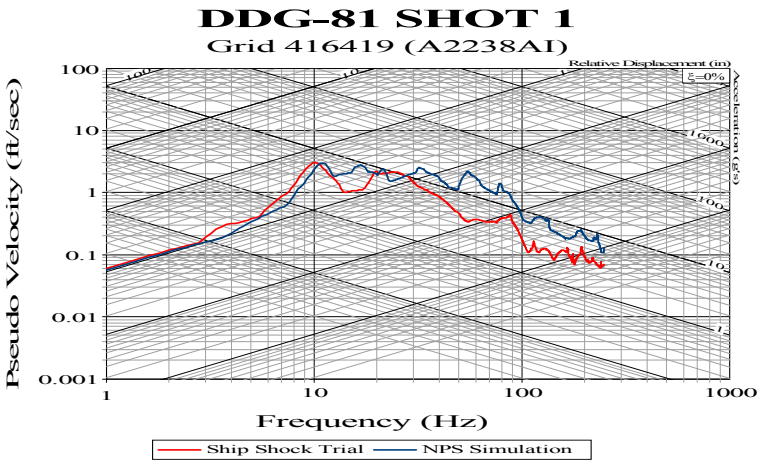

Figure 60. Port Mast Leg (MAST) Forward Outboard Corner

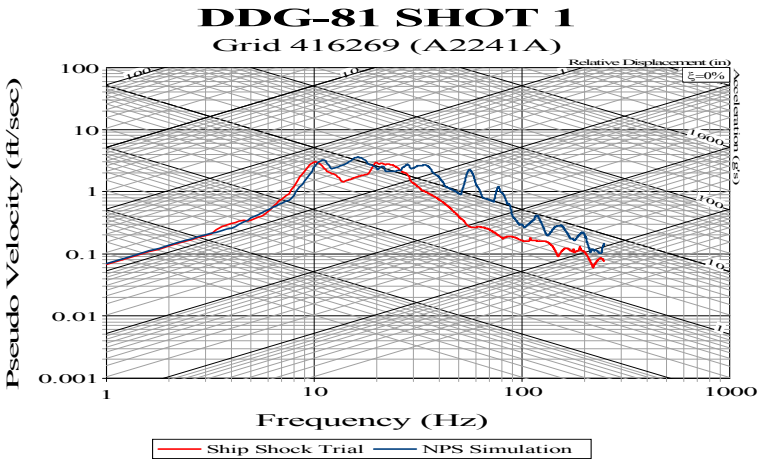

Figure 61. Stbd Mast Leg (MAST) Forward Outboard Corner

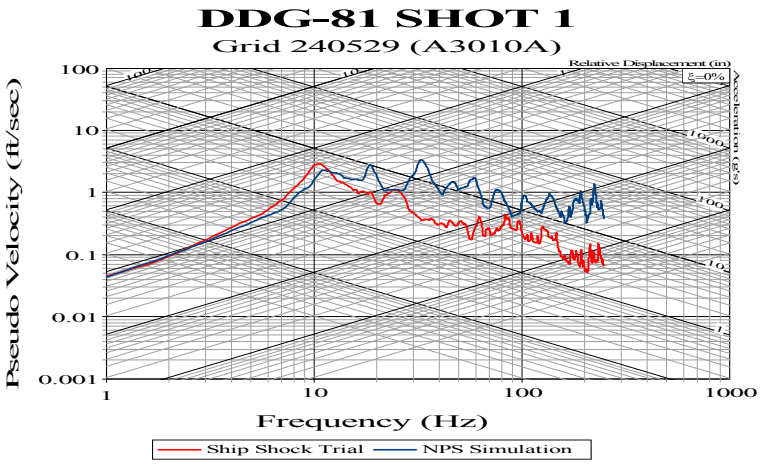

Figure 62. Central Control Station (1-268-0-C) Deck Sensor

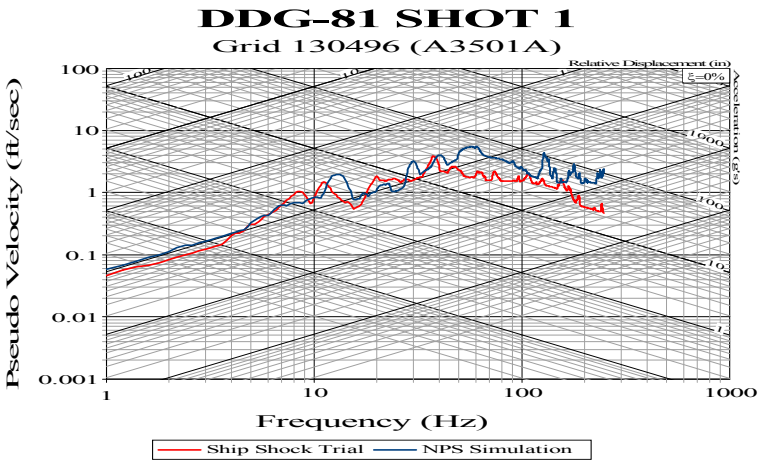

Figure 63. Combat Systems Equipment Room #1 (2-053-1-C) Deck Sensor

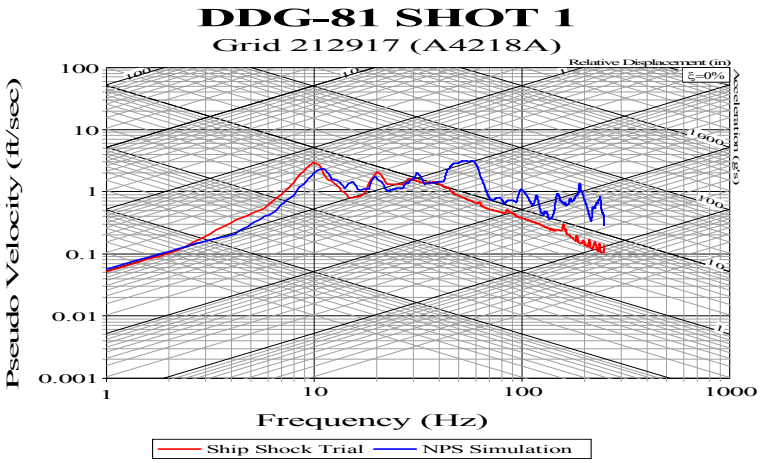

Figure 64. Combat Systems Maintenance Center (01-130-0-Q) Deck Sensor

B. SHOT 2

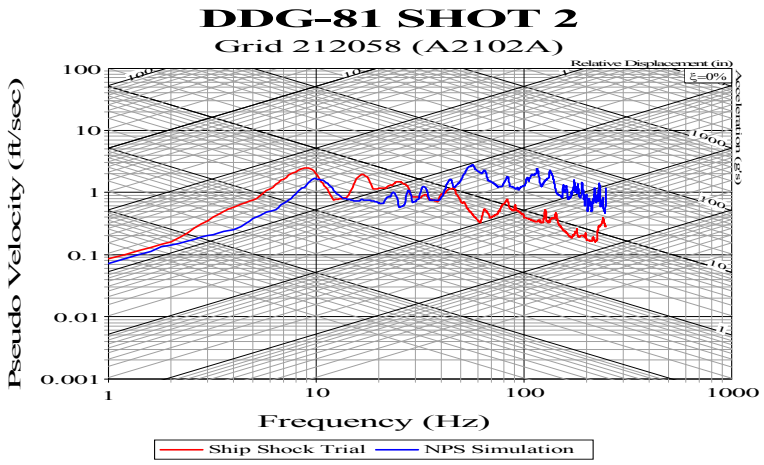

Figure 65. Combat Information Center (1-126-0-C) Deck Sensor FM 126

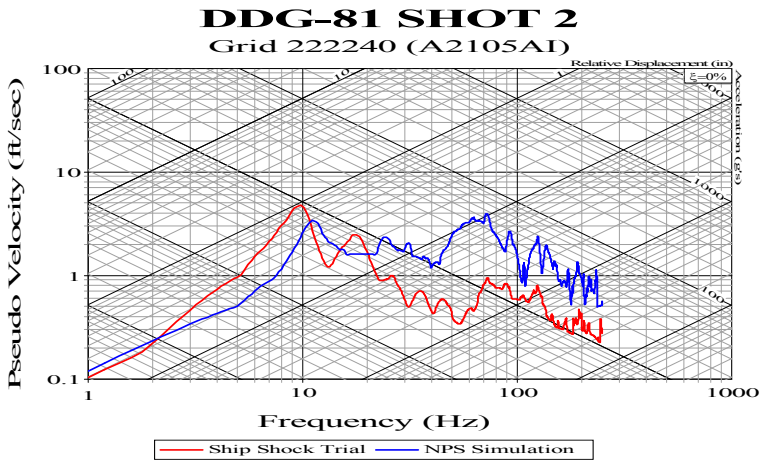

Figure 66. Combat Information Center Annex (1-126-0-C) Deck Sensor FM 174

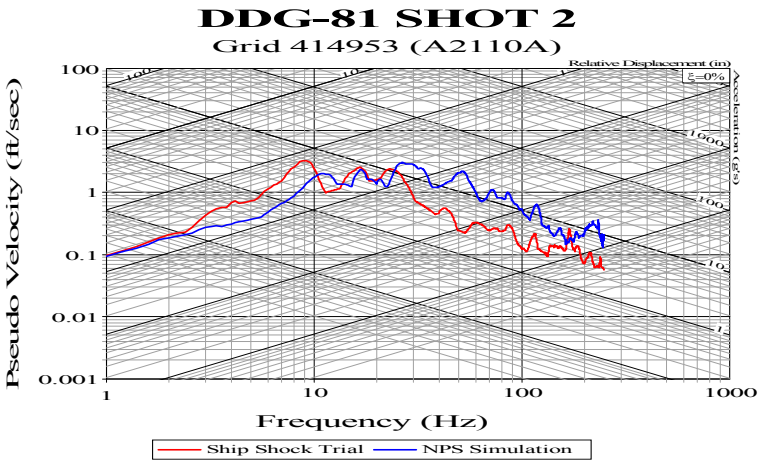

Figure 67. Radar Room #1 (03-128-0-C) Bulkhead Sensor

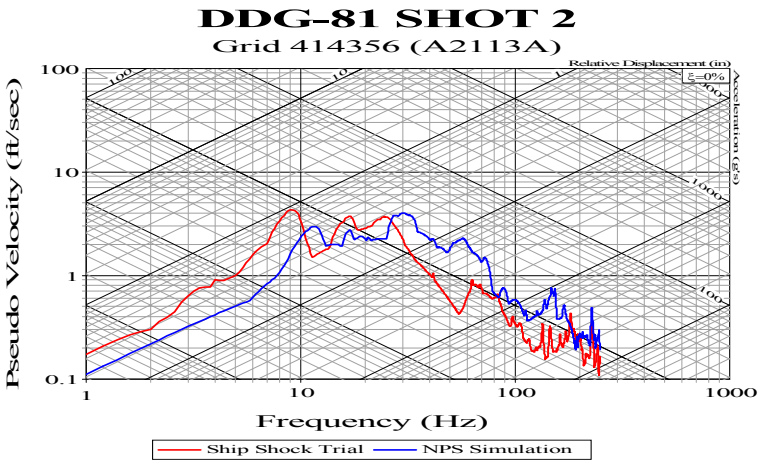

Figure 68. Passage Way (02-133-1-L) Overhead Sensor FM 142

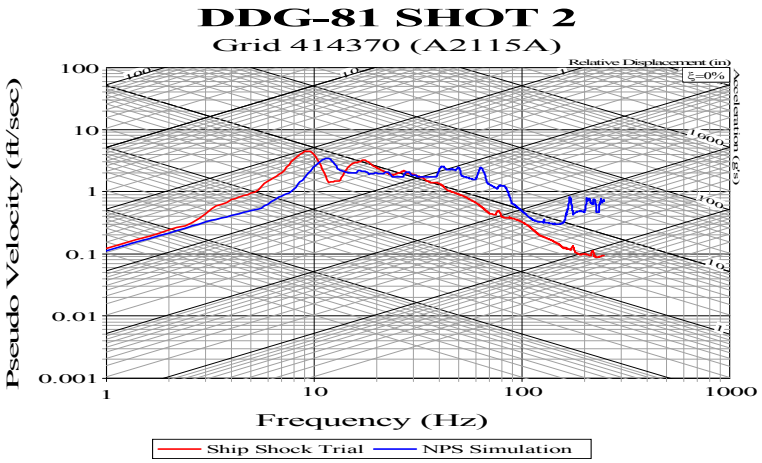

Figure 69. Radar Room #2 (03-142-0-C) Deck Sensor

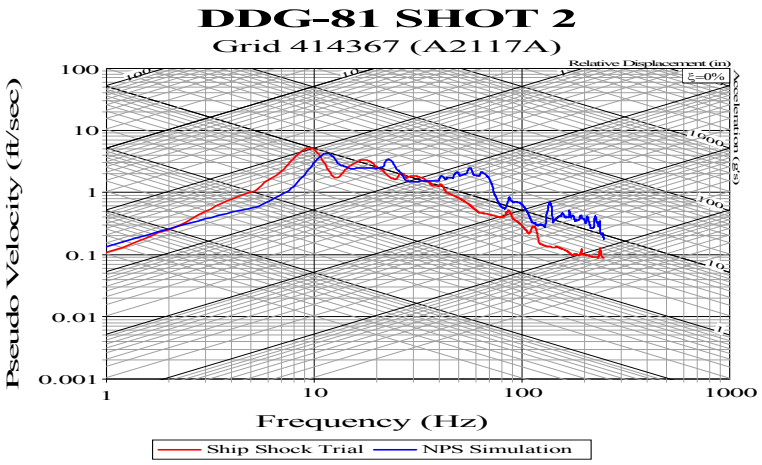

Figure 70. Radar Room #2 (03-142-0-C) Deck Sensor FM 174

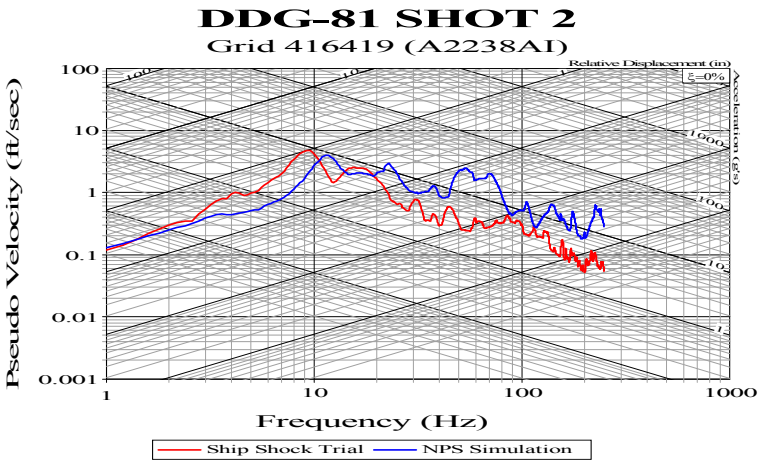

Figure 71. Port Mast Leg (MAST) Forward Outboard Corner

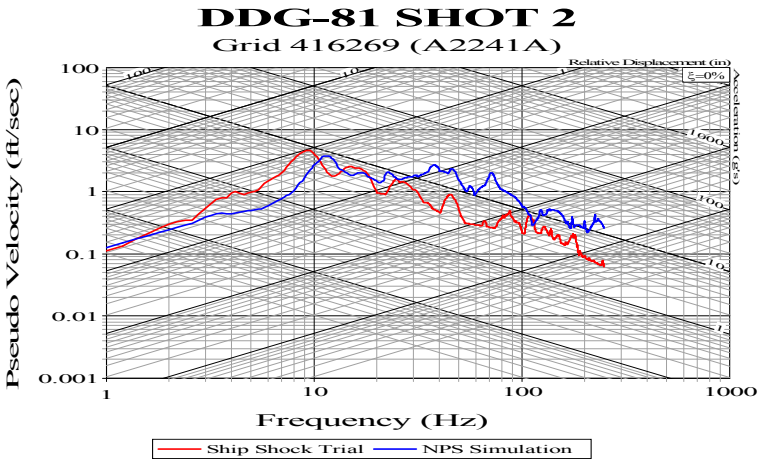

Figure 72. Stbd Mast Leg (MAST) Forward Outboard Corner

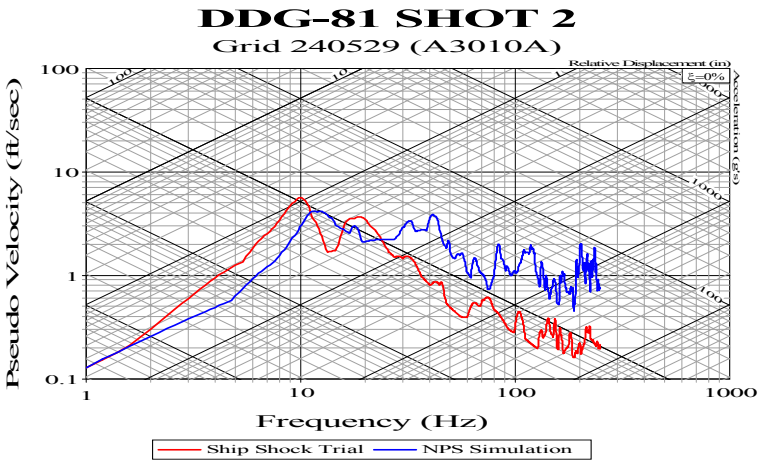

Figure 73. Central Control Station (1-268-0-C) Deck Sensor

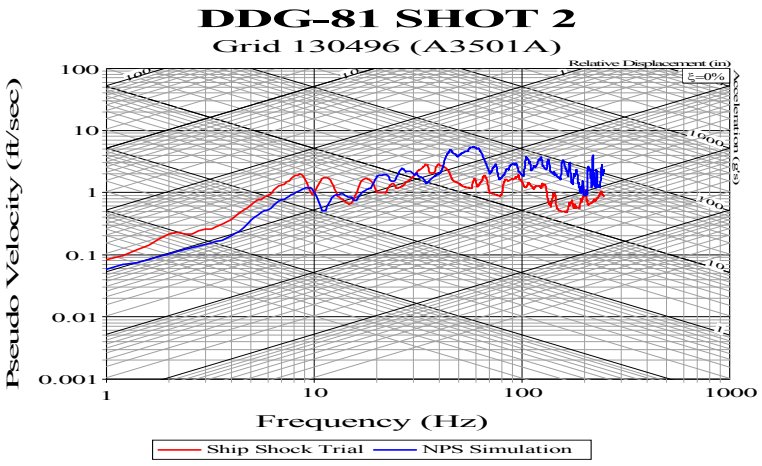

Figure 74. Combat Systems Equipment Room #1 (2-053-1-C) Deck Sensor

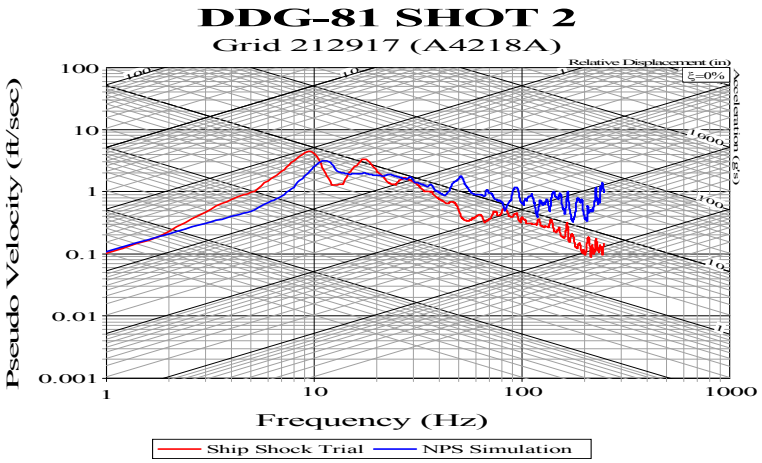

Figure 75. Combat Systems Maintenance Center (01-130-0-Q) Deck Sensor

C. SHOT 3

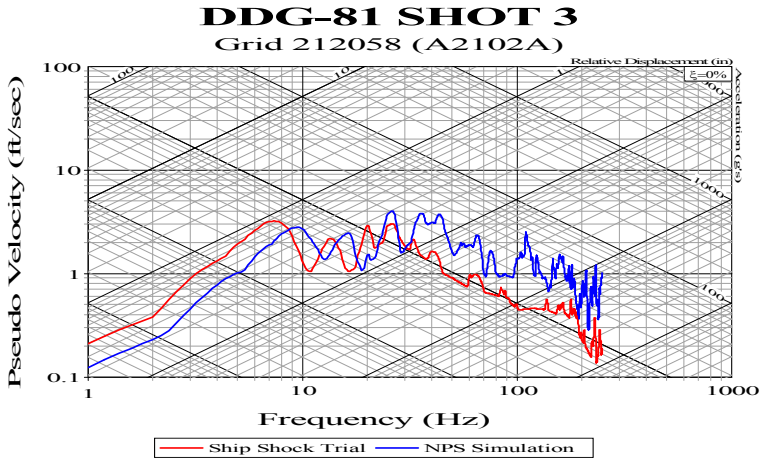

Figure 76. Combat Information Center (1-126-0-C) Deck Sensor FM 126

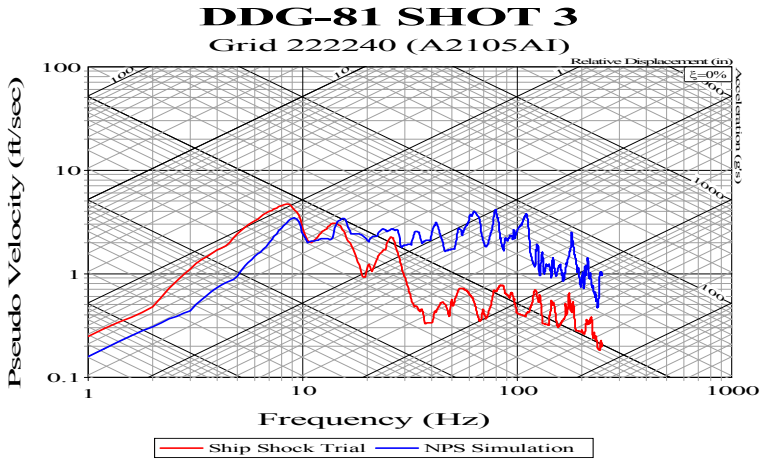

Figure 77. Combat Information Center Annex (1-126-0-C) Deck Sensor FM 174

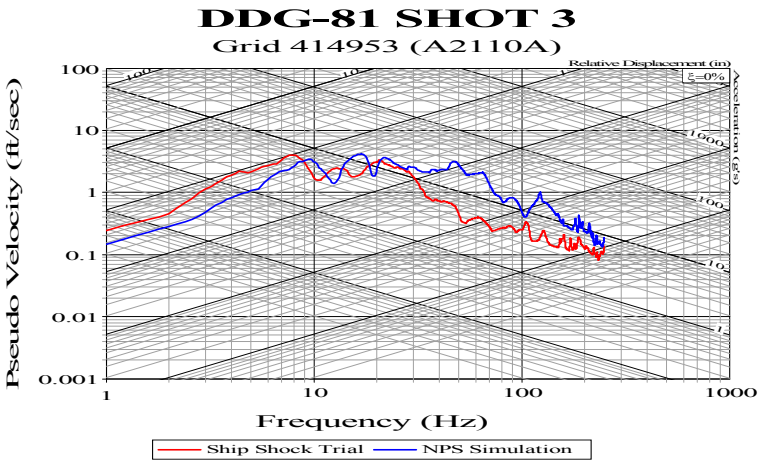

Figure 78. Radar Room #1 (03-128-0-C) Bulkhead Sensor

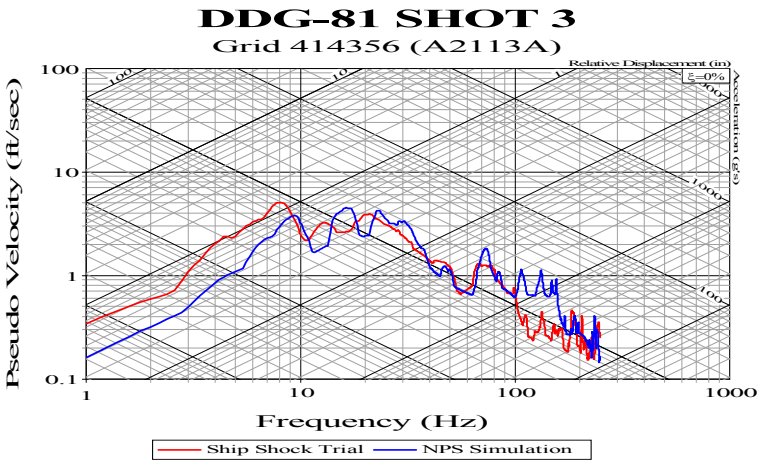

Figure 79. Passage Way (02-133-1-L) Overhead Sensor FM 142

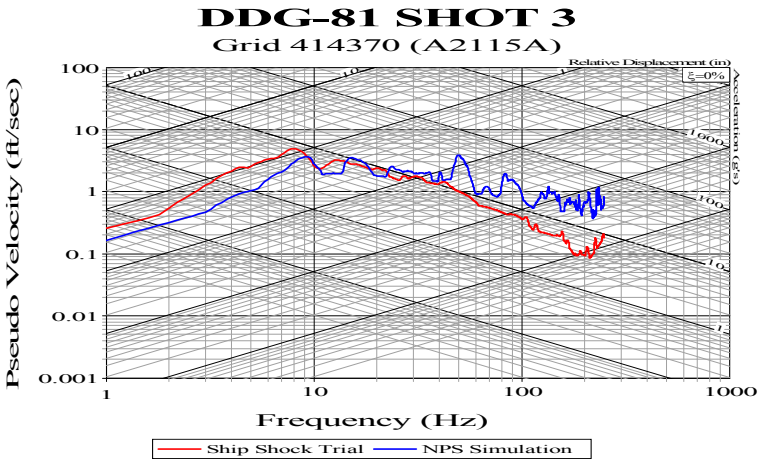

Figure 80. Radar Room #2 (03-142-0-C) Deck Sensor

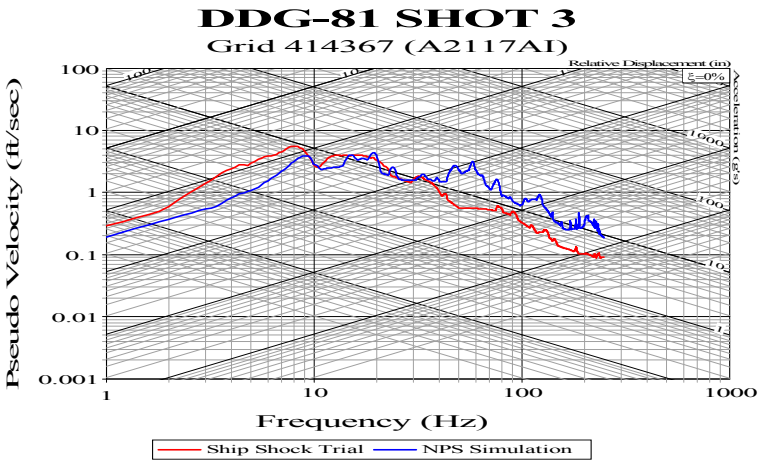

Figure 81. Radar Room #2 (03-142-0-C) Deck Sensor FM 174

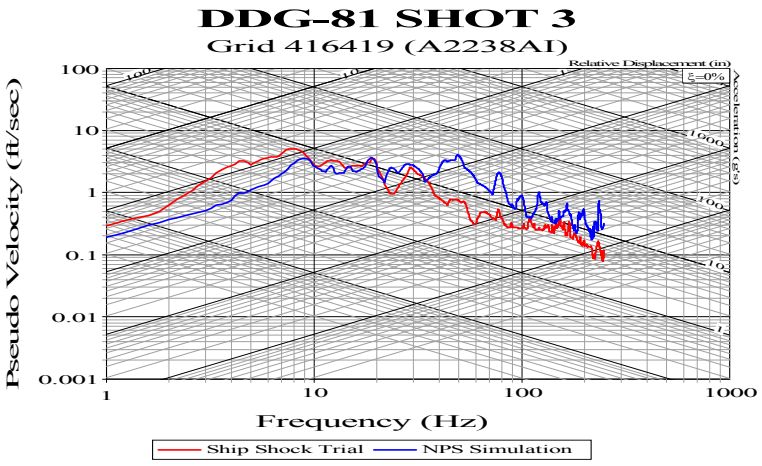

Figure 82. Port Mast Leg (MAST) Forward Outboard Corner

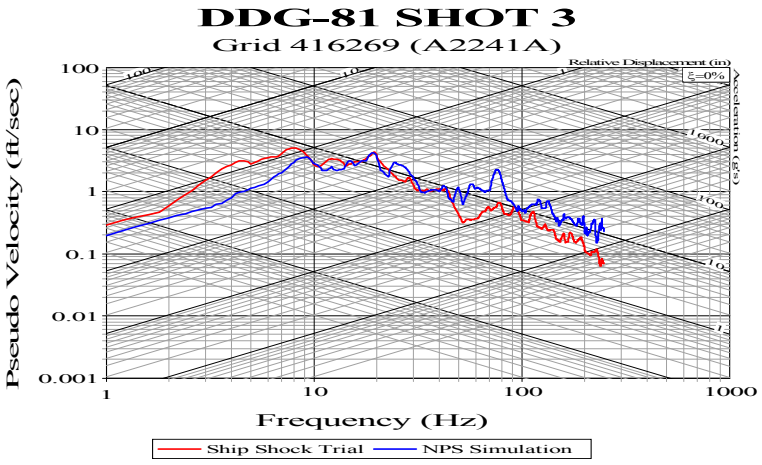

Figure 83. Stbd Mast Leg (MAST) Forward Outboard Corner

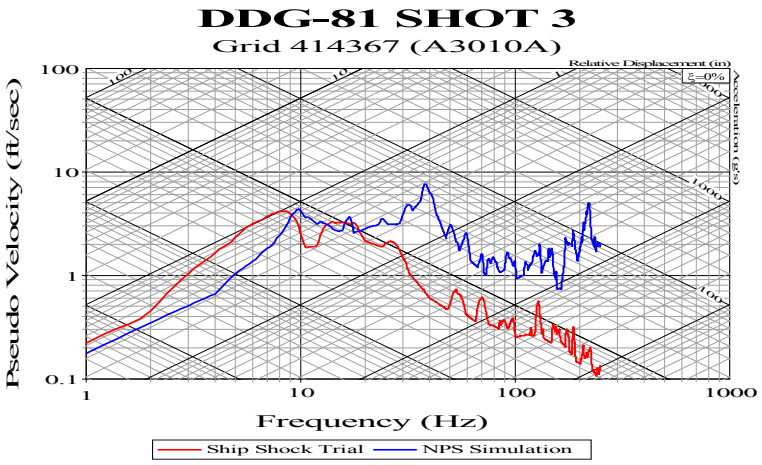

Figure 84. Central Control Station (1-268-0-C) Deck Sensor

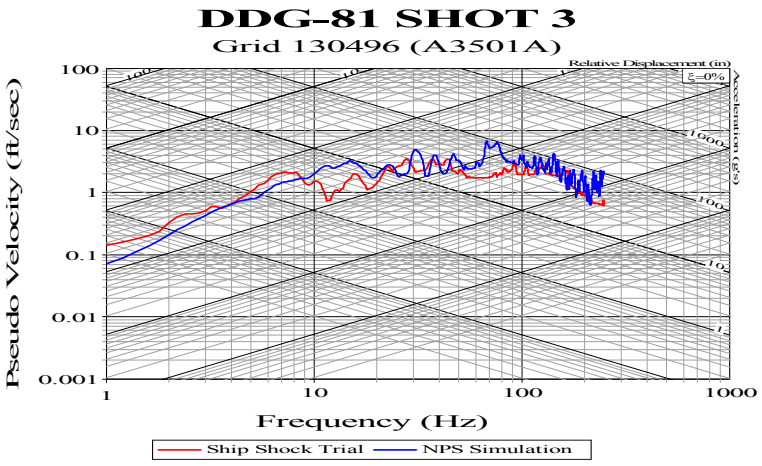

Figure 85. Combat Systems Equipment Room #1 (2-053-1-C) Deck Sensor

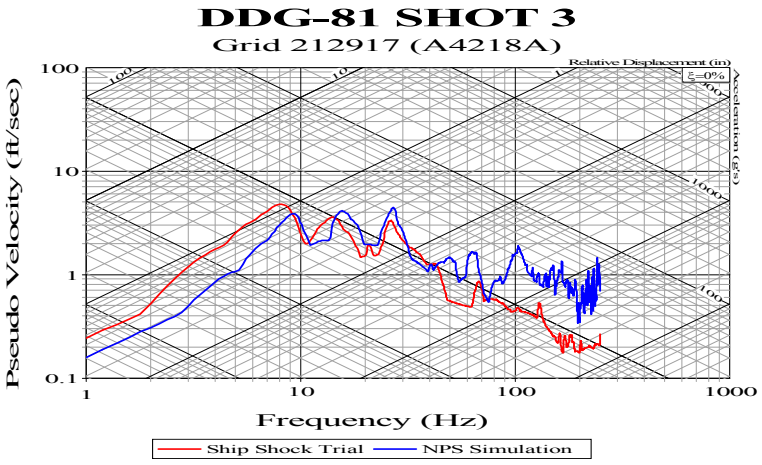

Figure 86. Combat Systems Maintenance Center (01-130-0-Q) Deck Sensor

APPENDIX C. MATLAB DATA PROCESSING ROUTINES

A. NODE-SENSOR IDENTIFICATION

The following program code was written using MATLAB. The purpose of this program is to compute the distance between nodes and sensors, then to select a node-sensor pair that is closest to each other.

```
%LT Doug Petrusa, USCG
%This program loads into memory the x,y, and z position of each node and
%each sensor.  It then calculates the distance formula for between each
%node and each sensor and stores that information in a Matrix "d."  Using
%the "min function" in MATLAB the smallest distance between the two is
%selected and stored in "locate" and "match".  Post Processing in Excel is
%needed since the Sensor numbers need to be added.
clear all;close all;clc;
load sensor_node;
tic
% Node=rand(2500,4);  smaller matrix to trouble shoot code
% Sensor=rand(100,4); smaller matrix to trouble shoot code
 d=zeros(length(Node),length(Sensor));
for i=1:length(Node)
   for j=1:length(Sensor)
      d(i,j)=sqrt((Node(i,2)-Sensor(j,2))^2+(Node(i,3)-Sensor(j,3))^2+(Node(i,4)-Sensor(j,4))^2);
   end
end

[closest index]=min(d);
locate(:,2)=closest';
locate(:,1)=index';
A=locate(:,1);
B=Node;
for p=1:length(A)
   match=B(A,:);
end
match(:,5)=locate(:,2);
toc
```

B. POLYNOMIAL DRIFT COMPENSATION

In an effort to improve data correlation between computer simulation and actual experimental results we have been using the Drift Compensation Function built into UERD Tools. This method has proven effective to remove significant drift from the sensors time history plot.

However in many cases the Drift Compensation function in UERDtools seems to drag the final data point in the time history plot back to equilibrium. Also, this function requires a minimum of 1000 msec's to operate.

Using simple Linear Algebra and Statistical Theory I have written a very simple algorithm which implements least squares polynomial curve fitting. This fitted curve represents the actual drift or error. Then subtracting the drift curve away from the sensor a corrected time history curve is obtained.

In Mathematical terms:

The basic Linear Algebra Equation:

$$\mathbf{A}\underline{x} = \underline{b}$$

Where **A** is a matrix and $\underline{x}$ and $\underline{b}$ are column vectors respectively. Substituting this equation in terms of x and y data from time history plots, $\underline{b}$ becomes the y (response) vector and $\underline{x}$ remains as the x (time-independent) vector. Matrix **A** will serve as a function operator, therefore our new equation is $\mathbf{A}\underline{x} = \underline{y}$. In most applications x is solved by a number of different algorithms, (eg $\mathbf{A}^{-1}\underline{b}$, LU, QR, rref…).

In least squares curve fitting we do not solve the above equation. Instead we modify the terms and generate an **A** matrix from our $\underline{x}$ data. In block matrix terms $\mathbf{A} = [\underline{a}^{(1)}\ \underline{a}^{(2)}\ \underline{a}^{(3)}]$ the first column vector of the **A** matrix is the individual terms of the original $\underline{x}$ vector squared ($\underline{a}^{(1)} = \underline{x}.^2$). The second column vector of A is the original $\underline{x}$ vector ($\underline{a}^{(2)} = \underline{x}$). The third column vector of the A matrix is a vector of ones ($\underline{a}^{(3)} = \underline{1}$). The $\underline{b}$ vector still remains unchanged.

Since the Matrix has three columns and the solution vector is a column of coefficients for a 2^{nd} degree polynomial our solution vector will have three unknowns. Our polynomial has the standard coefficients of $p(x) = ax^2 + bx + c$. Therefore let's name our new unknown vector $\underline{p}$. The newly formed equation is now:

$$\mathbf{A}\underline{p} = \underline{y}$$

Unfortunately this equation can't be solved on most, if not all occasions due to singularity. Therefore we will use the normal equations of Linear Algebra to get a least squares solution. This equation looks like the following:

$$\mathbf{A}^T\mathbf{A}\underline{p} = A^T\underline{y}$$

By left multiplying each side of the equation with the transpose of the A matrix we will now be left with a much smaller equation. Dimensionally this equation now takes the shape of a (3 by 3) (3 by 1) = (3 by 1) which is very easy to solve and leaves us with the desired polynomial coefficients.

With the new polynomial coefficients evaluated at every time step (evaluated along the x vector) a trend will be displayed. By subtracting this trend from the original time history response vector a drift compensated time history vector is generated.

This algorithm can easily be converted to fit a 3^{rd}, 4^{th}, $5^{th.}$…n^{th} degree polynomial by adding columns to the **A** matrix. Also, the other advantage is that only three data points are needed, not 1000. The following program code was written in MATLAB.

```
%LT Doug Petrusa
%NPS Shock Team
%Drift Compensation using Linear Algebra Least Squares Polynomial
%Curve Fitting.

sensor_data=textread('VA7008A.eu.asc'); %Sensor A7008A integrated and converted to ASCII
drift_data=textread('UERD_data.asc'); %Data Drift Compensated in UERD Tools
sensor_data2=textread('V2009VI.asc');%Sensor V2009VI converted to ASCII
drift_data2=textread('V2009VI_drift.asc'); %Data Drift Compensated in UERD Tools
%Break Data in x anmd y components - not necessary but allows for easy understanding of code

x=sensor_data(:,1); % x vector - Time in msec
y=sensor_data(:,2); % y vector - Velocity response in (ft/sec)

%Create the Matrix needed for Ax=b, Standard Linear Algebra Equation
A=[x.^2 x ones(length(x),1)];
%Program could easily be made a cubic fitting program by adding this line
%of code instead of the above line:
%A=[x.^3 x.^2 x ones(length(x),1)];

%Solve for polynomial coeff's using the Normal Equations (A'*A)x=A'b
%Coeff's to fit the Standard Polynomial equation: p(x)= ax^2 + bx + c
coeff=(A'*A)\(A'*y);

%Evaluate the newly created polynomial at each data point
curve_fit=polyval(coeff,x);

%Subtract away the curve
drift_comp=(y-curve_fit); %This is the newly compensated curve

%Plotting Commands
figure(1)
plot(x,drift_comp,'r')
grid on;
xlabel('Time (msec)')
ylabel('Velcity (ft/sec)')
title('Drift Compensation Methods')
hold on
plot(x,y,'k')
plot(drift_data(:,1),drift_data(:,2),'b')
legend('Least Squares Method','Sensor Data', 'UERD Tools Algorithm',0)
```

APPENDIX D. UERD TOOLS PROCESSING COMMANDS

This appendix contains a brief description of several of the commands and functions used to expedite the post processing of the time history plots and the corresponding shock spectra plots. UERDtools is a powerful post processing software tool created by Mr. Paul Mantz at NSWC Carderock, MD. This program is a collection of popular algorithms frequently used by mechanical engineers (e.g. numerical integration, unit conversion, unit scaling, fast fourier transforms) in a Window's based environment. Without the use of this software, each of the steps taken to post process the data collected would have required a separate Fortran or MATLAB code. The Input/Output interface to this program enabled fast and easy access to all of these algorithms.

A. COMMANDS

The following is a description of the major command needed to perform data post processing.

- *Calculus* – This command was utilized to integrate accelerometer data from the ship shock trial to velocity data by means of the trapezoid method. Differentiation is also accomplished by finite differencing.
- *Scale* – This command is extremely helpful in converting between units such as inches and feet quickly in one step. Conversions from English to SI units are also accomplished in the same manner. Also, the dependant axis can be scaled from seconds to milliseconds.
- *Combine Graphs* – When generating each of the time history curves presented in this thesis there were initially two separate plots. The first plot was typically the Ship Shock Trial data, and the second plot was the NPS Simulation data. This command would combine the two curves onto a single plot in one step. Automatically the plot was rescaled to properly display both curves, a legend is displayed at the bottom with distinct curve colors that can be preset by the user.

- *Filter* – Data filtering by means of two-pole Bessel functions was also used in the generation of the time history plots. In each plot shown in Appendix A, a low pass filter was set at 250Hz. In other words, all frequencies above 250 Hz were eliminated from the time history. Due to this fact no data is shown above 250 Hz in the shock spectra plots in Appendix B. This technique as described in Chapter III, removed the high frequency noise from the individual curves.

B. BATCH FILE FUNCTIONS

Most of the commands available in the UERDtools program can be automated by the use of a batch file operation. Instead of performing tasks such as the generation of one shock spectra plot from one time history plot, a batch file operation can create multiple plots simultaneously. By choosing a batch file command and selecting multiple time history plot files in a computer directory, the same command will be performed to each file.

The following batch file operations files were used to create all of the plots presented in this thesis:

- *Calculus* – Convert Ship Shock Trial data from Acceleration (g's) to Velocity (ft/sec).
- *Drift Compensation* – Corrects drift in Ship Shock Trial data (1000 msec time history required). Note: a different drift compensation method described in Chapter III was used in the preparation of the plots presented in this thesis.
- *Linear Interpolate* – Convert Simulation output (LS-DYNA) from ASCII text to UERDtools graph file with equal time steps (4e-6 seconds).
- *Scale* – Appropriately scale Simulation data x-axis from secs to msecs and y-axis from inches to feet.
- *Shift Time* – Used to match the start times of the Shock Trial Data curve and Simulation curve (typically 80 msec shift).

- *Sync Start Time* – Used after curves are combined on to one plot since the time steps vary between the two curves.
- *Trim Data* – Cut time histories from 2000 msecs to 500 msecs.
- *Filtering* – Low Pass 250 Hz curves
- *Find Russell's Error* – Creates a text files with the Russell's Error Factor and Gear's Error of each time history plot.
- *Shock Spectra* – Generates shock spectra plots from time history

THIS PAGE INTENTIONALLY LEFT BLANK

LIST OF REFERENCES

1. OPNAV Instruction 9072.2, "Shock Hardening of Surface Ships", 12 January 1987

2. Military Specification, MIL-S-901D, Shock Tests, High Impact Shipboard Machinery, Equipment and Systems, Requirements for, March 1989.

3. NAVSEA 0908-LP-000-3010A, Shock Design Criteria for Surface Ships, October 1994.

4. Schneider, N. A., "Prediction of Surface Ship Response to Severe Underwater Explosions Using a Virtual Underwater Shock Environment", Master's Thesis, Naval Postgraduate School, Monterey, CA, 2003.

5. Didoszak, J. M., "Parametric Studies of DDG-81 Ship Shock Trial Simulations", Master's Thesis, Naval Postgraduate School, Monterey, CA, 2004.

6. Harrington, M. J., Gibbs & Cox, Inc., "DDG-51 Flight IIA Shock Simulation", Presentation at the Naval Postgraduate School, August 2002.

7. Shin, Y. S. and Schneider N. A., "Ship Shock Trial Simulation of USS WINSTON CHURCHILL (DDG-81)", Presentation at the 74th Shock and Vibrations Symposium, October 2003.

8. Hart, D. T., "Ship Shock Trial Simulation of USS WINSTON S. CHURCHILL (DDG-81): Surrounding Fluid Effect", Master's Thesis, Naval Postgraduate School, Monterey, CA, 2003.

9. Shin, Y.S., "Naval Ship Shock and Design Analysis", Course Notes for Underwater Shock Analysis, Naval Postgraduate School, Monterey, CA 1996.

10. Finite Element Models of DDG-81, Gibbs & Cox, Inc., 2002

11. Ship Shock Trial Data of DDG-81, Naval Surface Warfare Center (NSWC) Carderock, MD 2001.

12. Shin, Y.S., "Ship-Shock Modeling and Simulation with Applications Using LS-DYNA/USA Code, and Review of DDAM", Naval Postgraduate School, July 2002.

13. USA+ Keyword User's Manual, Release 6.21, Anteon Corperation, Mystic CT, November 2003.

14. Shin, Y. S. "Damping Model Strategy for Naval Ship System", Report NPS-ME-03-003, Naval Postgraduate School, May 2003.

15. Russell, D. D., "DDG53 Shock Trial Simulation Acceptance Criteria", 69th Shock and Vibration Symposium, October 1998.

16. Electronic Mail Communication between Rutgerson, S. E., Naval Surface Warfare Center (NSWC) Carderock, MD and Author, 15 March 2004.

INITIAL DISTRIBUTION LIST

1. Defense Technical Information Center
   Ft. Belvoir, Virginia

2. Dudley Knox Library
   Naval Postgraduate School
   Monterey, California

3. Mechanical Engineering Department Chairman, Code ME
   Naval Postgraduate School
   Monterey, California

4. Naval/Mechanical Engineering Curriculum Code 34
   Naval Postgraduate School
   Monterey, California

5. Professor Young S. Shin, Code ME/Sg
   Department of Mechanical Engineering
   Naval Postgraduate School
   Monterey, California

6. Michael J. Harrington
   Gibbs and Cox, Inc.
   Arlington, Virginia

7. Tim Zimmerman
   Gibbs and Cox, Inc.
   Arlington, Virginia

8. Michael C. Winnette
   Underwater Explosion Research Department (UERD)
   Naval Surface Warfare Center - Carderock Division
   West Bethesda, Maryland

9. Constintine Constant
   Naval Sea Systems Command
   Washington, District of Columbia

10. CAPT David H. Lewis, USN
    Program Manager, Aegis Shipbuilding
    Naval Sea Systems Command
    Washington, District of Columbia

11. CDR Jeff Riedel, USN
    DDG-51 Class Post Delivery Manager (PMS 400PSA)
    Naval Sea Systems Command
    Washington, District of Columbia

12. Frederick A. Costanzo
    Underwater Explosion Research Department (UERD)
    Naval Surface Warfare Center - Carderock Division
    West Bethesda, Maryland

13. Steven E. Rutgerson
    Underwater Explosion Research Department (UERD)
    Naval Surface Warfare Center - Carderock Division
    West Bethesda, Maryland

14. LT Jay Main, USCG
    US Coast Guard Headquarters (G-SEN)
    Washington, District of Columbia